Coordination Chemistry Reviews 254 (2010) 487–505

Contents lists available at ScienceDirect

Coordination Chemistry Reviews

journal homepage: www.elsevier.com/locate/ccr

Review

Design of luminescent lanthanide complexes: From molecules to highly efficient photo-emitting materials

L. Armelao [a,*], S. Quici [b], F. Barigelletti [c], G. Accorsi [c], G. Bottaro [d], M. Cavazzini [b], E. Tondello [e,*]

[a] ISTM – CNR and INSTM, Dipartimento di Scienze Chimiche, Università di Padova, Via F. Marzolo 1, 35131 Padova, Italy
[b] ISTM – CNR, Via C. Golgi 19, 20133 Milano, Italy
[c] ISOF – CNR, Via P. Gobetti 101, 40129 Bologna, Italy
[d] IMIP – CNR and INSTM, Dipartimento di Scienze Chimiche, Università di Bari, Via Orabona 4, 70126 Bari, Italy
[e] Dipartimento di Scienze Chimiche, Università di Padova and INSTM, Via F. Marzolo 1, 35131 Padova, Italy

Contents

ARTICLE INFO

Article history:
Received 28 May 2009
Received in revised form 20 July 2009
Accepted 30 July 2009
Available online 7 August 2009

This article is dedicated to Fausto Calderazzo: an open minded and extremely upright person, an exemplary scientific guide.

ABSTRACT

The incorporation of luminescent lanthanide complexes in solid matrices with controlled structural organization is of widespread interest in materials science and has witnessed important improvements with the development of low-temperature *soft* chemistry solution processes, such as sol–gel. In this review, after an introductory part concerning some relevant aspects of the electronic and coordination properties of lanthanides, the prominent issues related to the design and synthesis of efficient luminescent antenna complexes, and their photophysical properties are presented. We describe the basic principles of ligands design to yield systems featuring a coordination site for the metal cation with appended suitable chromophores as sensitizers (two-component approach). When properly designed, these ligands are capable of forming highly luminescent complexes (overall sensitization yield, $\phi_{se} > 0.05$ in aqueous medium).

* Corresponding authors. Tel.: +39 049 8275236 (L. Armelao); Tel.: +39 049 8275220 (E. Tondello).
E-mail addresses: lidia.armelao@unipd.it (L. Armelao), eugenio.tondello@unipd.it (E. Tondello).

0010-8545/$ – see front matter
doi:10.1016/j.ccr.2009.07.025

Keywords:
Photoluminescence
Lanthanide antenna complexes
Light emitting silica layers
Inorganic/organic materials

The photophysical properties of these complexes together with the description of some emitting materials prepared are discussed in detail. In particular we focus the attention toward those complexes emitting in the visible region that can be used in the lighting industry (e.g. for the preparation of photo- and electro-luminescent materials) and for biological immunoassays. Subsequently, some selected results of our recent work concerning the synthesis of highly luminescent colour tunable films for applications in lighting and light conversion technologies are reported. Such materials have been obtained by combining the peculiar luminescence properties of Eu^{3+} and Tb^{3+} antenna complexes with optically transparent inorganic matrices. The notion is to create materials with innovative properties by integrating inorganic and organic components at nanoscale or molecular level. Due to the number of scientific publications in this field, this work is far from providing an exhaustive review on the previously performed research activities. For a more detailed discussion on these methodologies, the reader can refer to specific pertinent literature.

1. Introduction

1.1. Historical notes

"Lanthanons - these elements perplex us in our researches, baffle us in our speculations, and haunt us in our very dreams. They stretch like an unknown sea before us; mocking, mystifying and murmuring strange revelations and possibilities."

Sir William Crookes spoke these well-quoted words in an address to the Royal Society in February 1887, when all but three of the lanthanide elements had been isolated [1,2].

Composed of lanthanum and the 14 elements of the lanthanide series, the lanthanides (from the Greek word lanthaneien meaning "lying hidden" [3]) were once called the *rare-earth* metals. In fact, the scarcest of the lanthanides, thulium, is more abundant than either arsenic or mercury, and certainly no one thinks of these as rare substances. The most plentiful of the lanthanides, cerium, has an abundance of 46 ppm, greater than that of tin. If, on the other hand, rarity is understood not in terms of scarcity, but with regard to difficulty in obtaining an element in its pure form, then indeed the lanthanides are rare [4,5]. Because their properties are so similar, and because they are inclined to congregate in the same substances, the original isolation and identification of the lanthanides was an arduous task that took well over a century. Consequently, the terms "lanthanide series" or even "lanthanides" did not emerge for some time; in other words, scientists did not immediately know that they were dealing with a whole group of metals. As is often the case with scientific discovery, the isolation of lanthanides followed an irregular pattern, and they did not emerge in order of atomic number. Cerium was in fact discovered long before lanthanum itself, in the latter half of the eighteenth century. Not until 1875 was cerium actually extracted from an ore. It was named cerium in honor of Ceres, an asteroid between Mars and Jupiter discovered in 1801 [4,6]. There followed, a few decades later, the discovery of a mineral called ytterite, named after the town of Ytterby, Sweden, near which it was found in 1787. During the next century, most of the remaining lanthanides were extracted from ytterite [4,6], and with the discovery of lutetium (Lu) in 1907 the naturally occurring rare earths had all been isolated. The missing element number 61, promethium, was synthesized and characterized in 1947, completing the lanthanide series.

In the discovery of several lanthanide elements, luminescence has been instrumental and, in turn, these elements have always played a prominent role in lighting and light conversion technologies such as lasers, cathode-ray and plasma displays, light-emitting diodes, just to cite a few. More recently, it has been realized that the peculiar luminescent properties of the lanthanide ions could be exploited in applications ranging from biomedical to sensing areas and luminescence imaging; this led to most interesting developments in the coordination chemistry of these ions [3].

1.2. Forefront application fields of lanthanide complexes

Stable complexes of luminescent trivalent lanthanide ions have been since long under scrutiny in view of important applications [7], which are based on the exploitation of their magnetic [8–11] or luminescence features [3,12–14]. With regard to magnetism, the shift properties of paramagnetic Ln^{3+} complexes ($Ln \neq Gd$) can be exploited to enhance the well known properties of largely employed Gd^{3+} based contrast agents, commonly used in magnetic resonance imaging (MRI) [8]. In fact, a novel class of contrast agents based on the transfer of magnetization properties to the bulk water signal yield highly sensitive Ln^{3+} based probes for MRI. This approach, termed chemical exchange saturation transfer (CEST), allows the use of different contrast agents in the same MR-image, with each of them activated by selection of a characteristic irradiation frequency [8]. In order to overcome drawbacks associated with the low sensitivity of the MRI techniques, recent developments even include the use of metal containing nanosized systems to deliver a high concentration of contrast agent at the target tissue [15]. Another subject area where the magnetism of lanthanides can prove of use is that of the design of molecular magnetic compounds [9]. These can contain rare-earth ions coupled to d ions and organic radicals, and the properties of the devised materials may open ways to considerable development.

When the Ln^{3+} complexes exhibit intense luminescence, applications ranging from biomedical [7] to sensing areas [16] and optical imaging [11,17] become possible, which are based on the long-lived (milliseconds timescale) excited states of the lanthanide ions. Remarkably, the mostly studied complexes of Eu^{3+} and Tb^{3+} can exhibit quite intense visible line-like emission, as since long known from an exceptionally extended literature. The photophysical properties of near infrared (NIR) lanthanide emitters such as Sm^{3+}, Dy^{3+}, Pr^{3+}, Ho^{3+}, Yb^{3+}, Nd^{3+}, and Er^{3+} have been less well investigated in early times [18–22]. However, a massive interest in these complexes is registered in more recent times, which stems from their possible use in biomedical and telecommunication fields and for various photonic applications [23–29]. Actually, given that longer-wavelength emissions are more efficient to penetrate the human tissue than visible light, convenient medical diagnostic procedures can be conceived based on long-wave emitters. Similarly, NIR luminescence from ions such as Nd^{3+}, Yb^{3+} and Er^{3+} proves very useful when employed as optical signal amplifier in telecommunication network [30,31]. Regarding Nd^{3+}, since long it has found applications within laser systems [32,33]. Similarly, useful lasing properties are observed also for other Ln^{3+} centres [34].

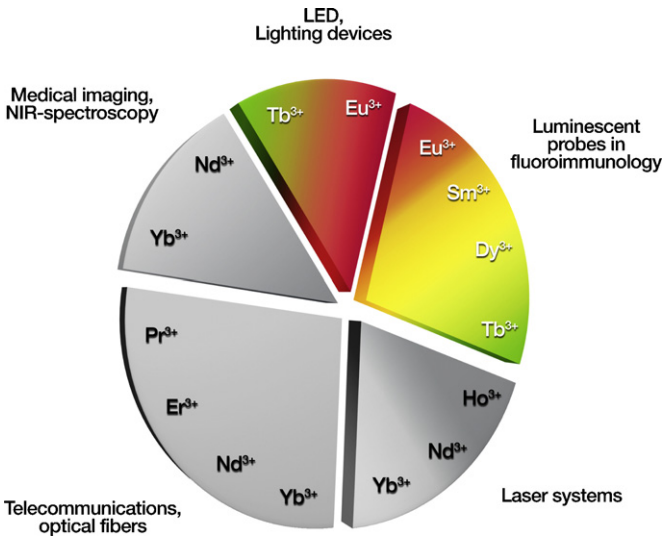

Fig. 1. Type of emission and related applications of lanthanides.

Various lighting applications are conceivable by using those Ln^{3+} centers that emit in the vis region. These are Tb^{3+}, Eu^{3+}, Dy^{3+}, and Sm^{3+} that, coupled with suitable antennas, can be incorporated in stable and transparent inorganic hosts, among others silica layers [35,36], and will be discussed in the following in some detail.

A schematic representation of the type of emission and of some major areas of application of lanthanides is evidenced in Fig. 1.

In this review we describe the basic principles of ligands design to yield systems featuring a coordination site for the metal cation with appended suitable chromophores as sensitizers (two-component approach). When properly designed, these ligands are capable of forming highly luminescent (overall sensitization yield, $\phi_{se} > 0.05$ in aqueous media) Ln^{3+} complexes. The photophysical properties of these complexes together with the description of some emitting materials prepared by us will be discussed in detail. In particular we focus the attention toward those complexes emitting in the visible region that can be used in the lighting industry (e.g. for the preparation of photo- and electro-luminescent materials) and for biological immunoassays.

2. Electronic properties and coordination number of lanthanide complexes

The fifteen elements from lanthanum to lutetium feature electronic configurations ranging from $[Xe]4f^0 5d^1 6s^2$ for La to $[Xe]4f^{14}5d^1 6s^2$ for Lu. The fourteen 4f electrons are added with some irregularities in the case of the atomic electronic configuration, while the progression is perfectly regular from $4f^1$ to $4f^{14}$ in the Ln^{3+} ions (Ln is the generic symbol of lanthanide elements). This particular electronic configuration is responsible for the constancy of lanthanide physical–chemical properties such as the oxidation state, the redox potentials and the ionic radii [37]. All of this results in a very similar chemistry which makes their separation very complicate [38]. The Ln elements all show a stable +3 oxidation state, which is the net charge that strikes the best balance between the ionization energy cost and the lattice-energy or solvation-energy stabilization of the ion. The potential for the Ln^{3+}/Ln^0 reduction is around −2.3 V *vs.* NHE (normal hydrogen electrode). Among the lanthanides, departure from the +3 oxidation state occurs for those elements that can approach the $4f^0$, $4f^7$ or $4f^{14}$ configurations. In these cases +2 or +4 oxidation states can be stabilized. For example Ce, Pr and Nd (just past $4f^0$) and Tb and Dy (just past $4f^7$) show the +4 oxidation state; Sm and Eu (just short of $4f^7$) and Yb (just short of $4f^{14}$) show the +2 oxidation state. Ce is the only rare-earth element for which molecular precursors in the +4 oxidation state are available [39], since for Pr, Nd, Tb and Dy the +4 oxidation state is observed only in the solid state.

For the lanthanides, the incomplete shielding of the nucleus by 4f electrons leads to a smooth contraction from $Z = 57$ to 71; thus a larger effective core charge contracts and stabilizes the 5p, 5d, and 6s orbitals [23]. This trend is known as the *lanthanide contraction* and it has some chemical effects of interest. The radii of the Ln^{3+} ions show a steady decrease from La^{3+} (1.17 Å) to Lu^{3+} (1.00 Å) [40,41]. Moreover, the radius of the main group Y^{3+} ion (1.04 Å) falls between those of Ho^{3+} and Er^{3+} and its chemistry closely resembles that of the late lanthanides [39]. The 4f electrons are shielded by the $5s^2$ and $5p^6$ orbitals and for the complexes they are scarcely available for covalent interaction with the ligands. Hence interactions are largely of electrostatic nature and the geometry of the Ln^{3+} complexes is determined by steric factors rather than electronic ones [42]. As a consequence, the Ln^{3+} complexes of the same ligand are all isostructural. Due to their small size, Ln^{3+} ions have a high surface positive charge density so that they behave as hard Lewis acids. Accordingly, they strongly coordinate ligands having highly electronegative donor sites (hard Lewis bases), in the order: $F^- > HO^- > H_2O > NO_3^- > Cl^-$ [43].

The coordination numbers of Ln^{3+} are in the range 3–12 depending on the steric demand of the ligand, with 8 and 9 as the most frequently observed. Aqua ions found in crystalline compounds are generally 9 coordinated with the tricapped trigonal prism being the favoured structure [44]. The $[Ln(H_2O)_n]^{3+}$ ions in aqueous solution are either 8 or 9 coordinated but this may vary with ionic strength and concentration [45]. The coordination number, in 1 M perchlorate solution, appears to change from 9 for larger Ln^{3+} ions (earlier elements of the series) to 8 for smaller ones (at the end of the series). The elements in the middle, such as Sm^{3+}, show either 8 or 9 water molecules in the first coordination sphere [46,47]. Very low coordination numbers, e.g. 3 or 4, have been observed with bulk ligands such as bis(trimethylsilyl)amide or bis(isopropyl)amide [48,49].

3. Spectroscopy of antenna–lanthanide complexes

The electronic spectra of lanthanide-doped single crystals and lanthanide salts can be interpreted within the frame of the Russel–Saunders coupling scheme [50]. This in principle should be strictly valid for light atoms whereas the lanthanides actually are not, given that they display moderately large spin–orbit coupling constants, e.g. $\zeta = 556$ and 1153 cm^{-1} for lanthanum and lutetium respectively [51]. The luminescence spectra show groups of narrow lines ascribed to transitions inside the 4f shell, that in solution can somewhat broaden in bands. Each small line within a group corresponds to a transition between two $^{2S+1}L_J$ free ion levels (J-manifold). Within the Russel–Saunders coupling scheme, for L = 0, 1, 2, 3, 4, 5, and 6 the spectroscopic terms are labelled S, P, D, F, G, H, and I. In most cases, the lanthanide ions have ground states with a well-defined value of J, with the next J state not thermally accessible at room temperature. For the lanthanide cations we are more interested here in view of the optical applications discussed later, the electronic ground levels are $^6H_{5/2}$ (Sm^{3+}), $^7F_0$ (Eu^{3+}), $^8S_{7/2}$ (Gd^{3+}), $^7F_6$ (Tb^{3+}), and $^6H_{15/2}$ (Dy^{3+}) [50]; to notice that electronic transitions are intraconfigurational in character and are only allowed between $^{(2S+1)}L_J$ levels for $\Delta L = \pm 1.0$ or $\Delta J = \pm 1.0$.

Given that the Ln^{3+} centers cannot efficiently absorb light (the extinction coefficient for such trivalent cations is $\varepsilon \approx 1$–$10\ M^{-1}\ cm^{-1}$) [52], the way of choice to sensitize their luminescence is to employ chromophores (L) as antennas for light absorption; for most organic chromophores in the UV region, $\varepsilon \approx 10^4$–$10^5\ M^{-1}\ cm^{-1}$ [51,53]. In this case, the following sensiti-

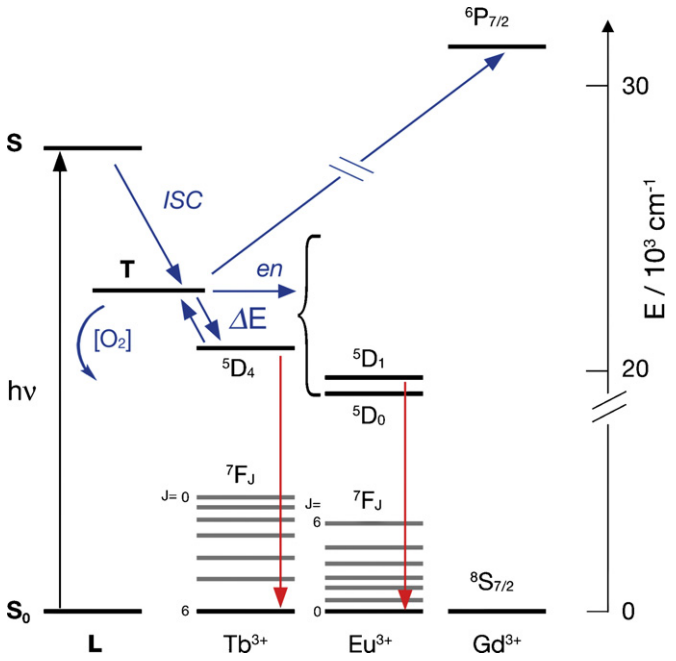

Fig. 2. The antenna effect for sensitization of the luminescence in some lanthanide cations (selected levels are displayed); blue arrows indicate non-radiative processes, red arrows indicate radiative processes. As exemplified here for the Tb^{3+}, Eu^{3+}, and Gd^{3+} centres, three cases are encountered with regard to energy transfer (en) as regulated by the energy gap, ΔE, between the triplet level (T) of the chromophore (L) and the emitting level of the cation: (a) when $\Delta E \leq 1500\,cm^{-1}$ back energy transfer takes place and, as a consequence, O_2-effects (particularly intense in solution at room temperature given the long lifetime of the ligand triplet level) are observed, see text; (b) when $\Delta E \geq 1500\,cm^{-1}$ energy transfer is complete and (c) energy transfer is exothermic and does not take place.

zation steps take place: (i) population of the lowest-lying singlet excited state (S) of the organic chromophore, (ii) subsequent intersystem crossing (ISC) to its triplet level (T) and (iii) energy transfer (en) to the Ln^{3+} centre. The sensitization process can also be performed by chromophores from the vast area of the transition metal complexes [23,54–59]. A reference scheme for the sensitization process is provided in Fig. 2 [60–62].

The overall efficiency of Ln^{3+} sensitized emission (ϕ_{se}), consequent to the light absorption event, is therefore regulated by the intersystem crossing efficiency (ϕ_{ISC}), the energy transfer efficiency (ϕ_{en}), and the intrinsic metal centred (MC) luminescence quantum yield of the Ln^{3+} ion ($\phi_{lum}{}^{MC}$), Eq. (1a):

$$\phi_{se} = \phi_{ISC}\phi_{en}\phi_{lum}^{MC} \quad (1a)$$

$$\phi_{lum}^{MC} = \frac{k_r}{k_r + k_{nr}} \quad (1b)$$

In water, in order to inhibit non-radiative deactivation *via* interaction with OH oscillators, the 8–9 coordination positions of Ln^{3+} must be conveniently shielded against the intervention of solvent molecules [63–66], Eq. (1b); k_r and k_{nr} are radiative and non-radiative rate constants, respectively. In this regard, comparison of luminescence results as obtained in water and deuterated water solutions allows the assessment of water binding. For Eu^{3+} and Tb^{3+} centers, this can be done by using the following equations where q (uncertainty ±0.5) is the number of coordinated water molecules and lifetimes (τ) are in ms [64,67].

$$q^{Eu} = 1.2\,(1/\tau_{H_2O} - 1/\tau_{D_2O} - 0.25) \quad (2a)$$

$$q^{Tb} = 4.2(1/\tau_{H_2O} - 1/\tau_{D_2O} - 0.06) \quad (2b)$$

Thus, the ligand system selected for the building up of the complexes must meet a number of requirements. These are related both to the needed structural features (complex stability and saturation of the coordination positions) and to the fact that, for maximizing the emission intensity, each of the three steps involved in the sensitization event must be optimized, Eq. (1a).

4. Design of luminescent lanthanide complexes

4.1. General criteria

The electronic, magnetic and photophysical properties of Ln^{3+} complexes strongly depend on the control of the coordination sphere of the metal. Accordingly, particular care should be paid to the design of ligands to optimize the property of interest. For instance, a review that describes the basic principles for the design of organic ligands for alkali and alkali-earth cations has been reported by Lehn in 1973 [68]. In this review the parameters to be considered to achieve the control over chemical, structural and thermodynamical properties of the complex, which in the end govern its functionality, are clearly described. Among these parameters the ligand topology (dimensionality, connectivity, shape, size, and chirality), the binding sites (nature, electronic properties, number, shape, arrangement), the layer properties (rigidity/flexibility and the lipophilicity/hydrophilicity ratios, thickness), the environment properties and counterions effect are particularly important. These general rules apply to any kind of ligand, independently of the metal cation, and are particularly important in the case of Ln^{3+} whose coordination is substantially based on Van der Waals electrostatic interactions and is similar to that of alkali-earth cations, in particular Ca^{2+}.

In general, the complex formation is the result of an attraction between a ligand and a metal cation and is associated with their partial or total desolvation. In other words the coordination sites of the ligand interact with the surface of the metal cation thus replacing partially or totally the first solvation sphere. From the thermodynamic point of view this process affords an increased entropy because of the desolvation step, while the enthalpy variation can be either positive or negative according to the difference between the energy of the bonds formed (ligand–cation) and the energy of the bonds broken (ligand–solvent; cation–solvent).

In the complexation of Ln^{3+} in aqueous solution the dehydration step is endothermic ($\Delta H > 0$) and represents an unfavourable energy contribution to the variation in Gibbs free energy so that the overall process is entropy driven. Therefore it is convenient to use polydentate ligands, which, because of the chelate effect, can overcome this difficulty and afford highly stable complexes even in aqueous medium.

In order to increase the thermodynamic stability of the complex, the Ln^{3+}-ligand interaction has to be maximized. Indeed, due to their hard character, Ln^{3+} cations show preference for hard binding sites having large electrostatic components so that anionic ligands such as carboxylates, phosphinates, phosphonates and β-diketonates are strongly recommended.

As it has been already stated, a luminescent Ln^{3+} complex is a multicomponent system in which the active components, namely: the metal cation, the antenna and the coordination site, are organized in a supramolecular structure. Consequently the choice of these components and their positioning in the overall structure are issues to be considered during the molecular design step in order to optimize the overall sensitization efficiency.

4.2. Choice of the lanthanide

The emission properties of the lanthanide cations cover a wide spectral range that spans from the UV (Gd^{3+}) to the visible: orange (Sm^{3+}), red (Eu^{3+}), yellow (Dy^{3+}), green (Tb^{3+}) and blue (Tm^{3+}) to

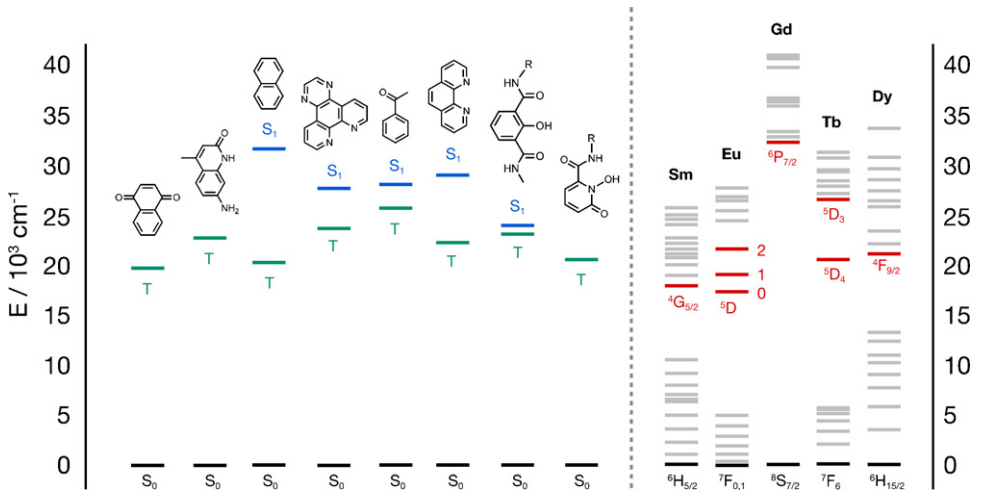

Fig. 3. Energy diagram of emissive levels of some lanthanide cations and chromophores: singlet states and triplet states of chromophores are evidenced in blue and green respectively, while relevant emitting states of some lanthanides are drawn in red.

the NIR (Yb^{3+}, Nd^{3+} and Er^{3+}). A simplified energy diagram of the emissive levels of Ln^{3+} cations emitting in the visible, together with the energies of singlet (blue) and triplet (green) excited states of some commonly used chromophores are reported in Fig. 3.

The lanthanides usually possess relatively long-lived excited states (microseconds to milliseconds time scale), which can undergo energy transfer to high frequency vibrational oscillators such as OH, NH and, to a lower extent, CH. As a consequence, the presence of these groups in the proximity of the metal favour thermal dissipation of the energy (vibronic coupling) which gives rise to quenching of the luminescence. In particular, the lower is the excited state energy of the Ln^{3+} ion the more efficient will be the deactivation by vibronic coupling, an effect termed "energy gap rule" [69,70]. Thus, with Ln^{3+} emitting in the NIR the emission is strongly reduced and in some circumstances it cannot even be observed when high frequency oscillators are present in the coordination site.

4.3. Choice of the antenna

The chromophore that promotes the sensitization of the lanthanide light emission is normally named "antenna" and is important in determining the emission intensity of the Ln^{3+} complex. In general the antenna can be any aromatic or hetero-aromatic highly π-conjugated system characterized by high efficiency of light absorption (high extinction coefficient ε) and high efficiencies of intersystem crossing and energy transfer processes. Among others, the efficiency of a chromophore to behave as sensitizer is related to the energy of its triplet excited state (Fig. 2), which should be at least 1850 cm^{-1} higher than the lowest emitting levels of the Ln^{3+} cation [71]. When the energy gap is higher the energy transferred from the triplet flows through non-radiative excited states of the metal until it reaches the emissive levels and the metal centred emission occurs. On the contrary a lower energy gap strongly limits the emission quantum yield because of thermal deactivation due to back energy transfer and O_2-quenching towards the chromophore triplet level (Fig. 2). The triplet energies of commonly used chromophores are reported in Table 1. Taking into account the rules mentioned above, it is unlikely that the same chromophore can efficiently acts as antenna for different Ln^{3+} cations. This is further complicated by the possible population of non-radiative excited states, such as ligand-to-metal charge transfer (LMCT), that can occur with apparently suitable ligands, thus resulting in non luminescent Ln^{3+} complexes. Another important point regards the excitation wavelength of the antenna that should be above ca. 350 nm to facilitate the use of inexpensive excita-

Table 1
Energy levels of commonly used chromophores[a].

Chromophore	Singlet (cm^{-1})	Triplet (cm^{-1})	λ_{max}, ε (nm, M^{-1} cm^{-1})	Ref.
2,2′-Bipyridine[b]			287, ~29,200	[74]
1,10-Phenanthroline	29,200	22,100	264, 33,900	[51]
2,2′:6′,2″-Terpyridine[b]			305, ~22,200	[75]
2,9-Dimethyl-4,7-diphenyl-1,10-phenanthroline[c]		21,200	274, 68,500	
Acetophenone	28,200	26,000		[51]
1,4-Naphthoquinone		20,200		[51]
8-Hydroxyquinoline[d]	~27,000		305, –	[76]
7-Amino-4-methyl-2-hydroxyquinoline (Carbostyril 124)		23,100		[51]
Tetraazatriphenylene[b]	29,000	24,000	340, ~4,000	[19]
Naphthalene	32,200	21,200	275, ~56,000	[51]
2-Hydroxyisophthalamide (IAM)	24,200	23,350		[77]
1-Hydroxypyridin-2-one (1,2-HOPO)		21,260		[78]

[a]For the solvents employed see the original works. [b]The luminescence properties of 2,2′-bipyridine (bpy) and 2,2′:6′,2″-terpyridine (tpy) free ligands, whose structure is far from being substantially rigid and close to planarity, are difficult to ascertain; on the other hand, for the huge amount of known complexes of these ligands, inspection of their LC singlet and triplet levels is difficult because of very fast deactivation towards lower lying levels of MLCT, MC and LMCT nature. As an approximation, the listed absorption data are drawn from UV absorption profiles of $[Ru(bpy)_3]^{2+}$ [74] and $[Ru(tpy)_2]^{2+}$ [75] respectively and are to be considered with some care. [c]Results from our laboratories. [d]The spectroscopic properties of free 8-hydroxyquinoline are heavily affected by photoinduced photoisomerization and solvation effects that result in a very weak or no emission [76], while for the complexes the same comments as in footnote (b) are likely to hold [79].

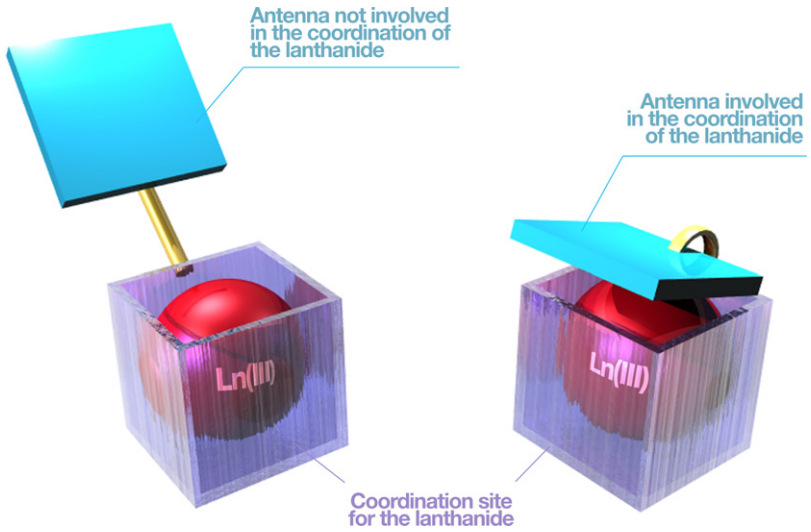

Fig. 4. Possible ways to position the antenna within the ligand.

tion sources and to avoid the use of expensive quartz optics, for instance in the immunoassay applications. According to the position and nature of the chromophore the energy transfer process can occur either by Förster [72] or Dexter [73] mechanisms. In order to ensure fast energy transfer a short distance between the sensitizer and the Ln^{3+} cations is obviously advantageous; the best results can be obtained when the antenna directly coordinates the metal centre. This situation has been mainly exploited with chromophores containing binding sites for the Ln^{3+} cation such as: aza-aromatic compounds (bipyridine, phenanthroline, azatriphenylene, terpyridine) or phenolate aromatics [2-hydroxyisophthalamide (IAM), 1-hydroxypyridin-2-one (1,2-HOPO)], Table 1. With these chromophores, in order to satisfy the coordination properties of the lanthanide ion, besides the nature of the binding sites, their relative position in the overall structure of the ligand becomes particularly important.

4.4. Choice of the coordination site

The coordination site is formed by a number of donor atoms or groups arranged in a covalently organized structure and capable of binding the metal cation strongly. According to the dimensionality, the coordination site can be: monodimensional as in the case of acyclic ligands which can be linear (podands) or branched (polypodands); bidimensional macrocyclic ligands (coronands), and tridimensional in macrobicyclic and macropolycyclic ligands (cryptands). As a consequence the complexes formed can be of chelate (podates) or of inclusion (cryptates) types. The degree of cation shielding depends on the length, flexibility and number and nature of binding sites in the case of podates, while with cryptates the nature and number together with the preorganization of binding sites are particularly important. The positioning of the antenna within the coordination site together with its physical and chemical properties are also very important for the preparation of highly luminescent Ln^{3+} complexes. This point can be addressed mainly in two ways: with the antenna subunits (i) covalently attached through a suitable spacer; or (ii) integrated into the coordination site structure. In this latter combination, which represents also the most suited one, the antenna directly participates in the building of the coordination site besides acting as sensitizer, Fig. 4. In the following we will examine a few useful approaches based on the use of different types of ligands and will illustrate the two-component approach employed by us.

4.5. Acyclic ligands

There are many examples of acyclic coordination sites that have been used for the preparation of luminescent lanthanide

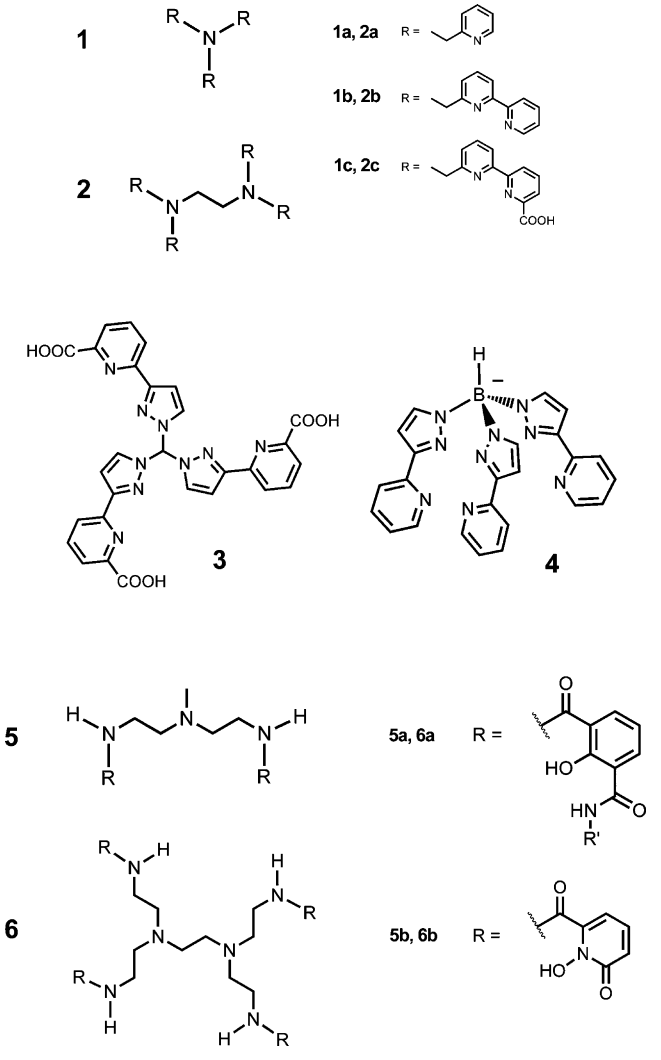

Fig. 5. Acyclic ligands employed for the preparation of luminescent Ln^{3+} complexes.

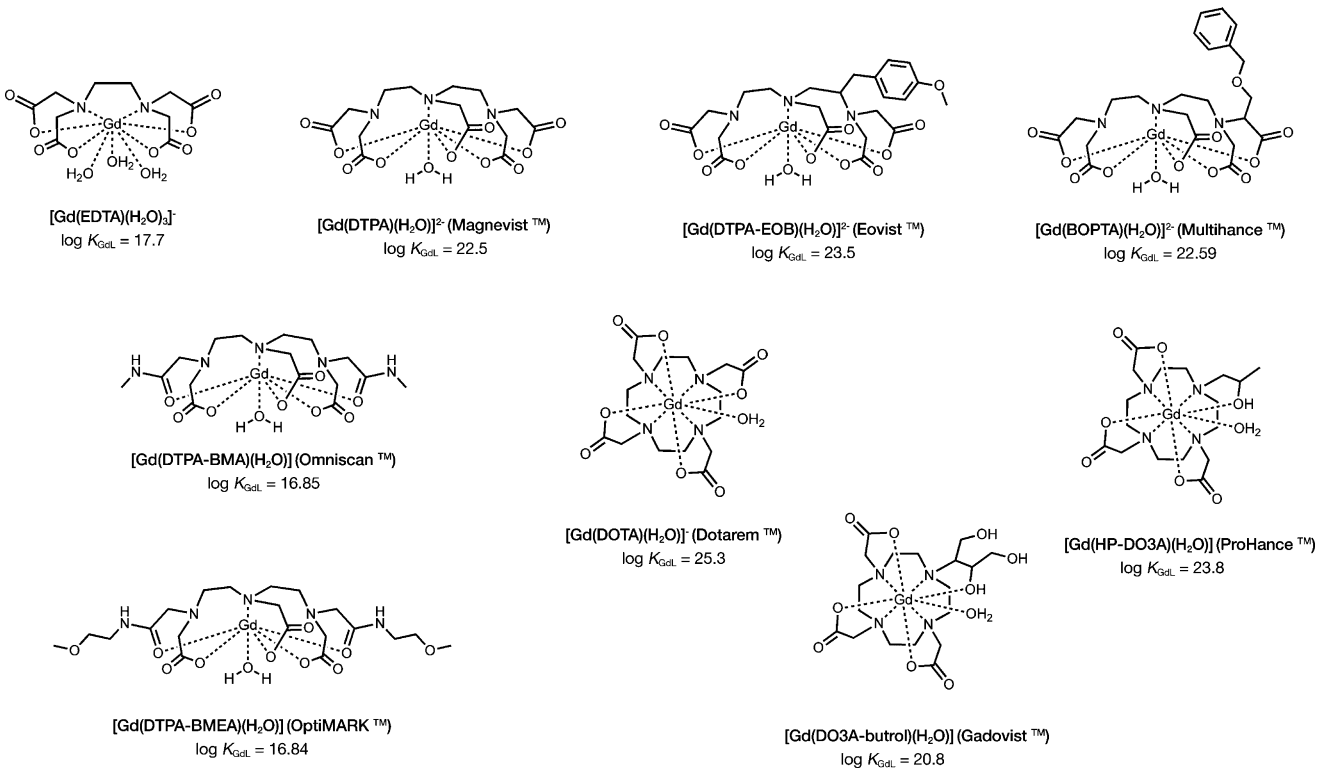

Fig. 6. Gd^{3+} chelates currently employed as MRI agents.

complexes. Among them particularly interesting are branched polypodands bearing a number of binding sites [80]. As stressed before in order to form stable complexes in aqueous solution, the donor atoms of the ligand should satisfy the demand of a hard Ln^{3+} cation and this condition can be readily fulfilled by the presence of hard and anionic donor sites such as carboxylates, phosphonates, phosphinates and β-diketonates that strongly coordinate to the highly positive metal cation. The structure of the ligand must be sufficiently flexible so that it can envelope the spherical Ln^{3+} cation as tightly as possible giving rise to a cryptate-like complex featuring very high thermodynamic and kinetic stabilities and a complete shielding of the metal centre "induced fit". In other words, in order to operate through an induced fit mechanism, the ligand should feature a number of binding sites higher or equal to the coordination number of the Ln^{3+} cation arranged to match precisely the coordination properties of the metal "predisposed ligand". The stability of the complex increases with ligands having anionic binding groups that strongly interact with the cation thus favouring the coordination of nitrogen and/or oxygen donor atoms, contained into the ligand structure, according to the well known "end group effect" that is a general concept in the design of highly efficient polypodands [80].

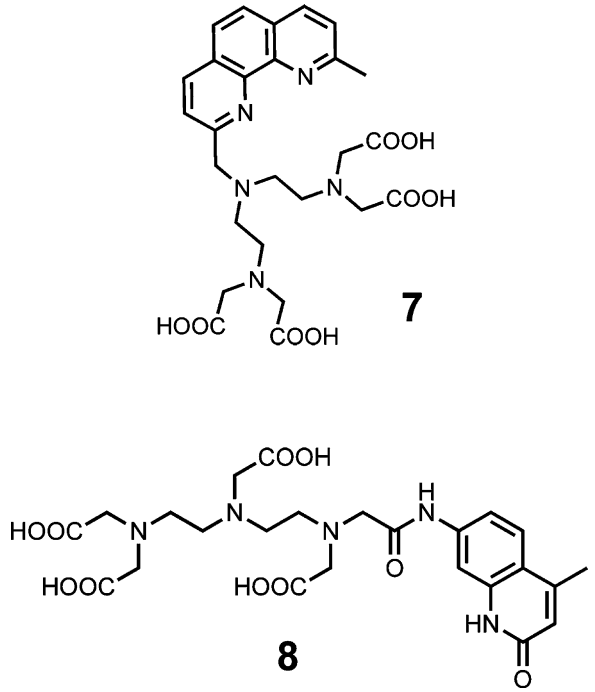

Fig. 7. Strongly chelating ligands used for the preparation of highly luminescent Eu^{3+} and Tb^{3+} complexes.

Most of the acyclic ligands used for the preparation of luminescent Ln^{3+} complexes contain a number of hetero-aromatic groups connected to various linkers that determine the architecture of the entire molecule. Nitrogen atoms of ethylendiamine and polyamine skeletons have been commonly used as linkers, while the heterocyclic subunits (pyridine, bipyridine, bipyridine carboxylate and so on) behave either as binding site and as antenna toward the lanthanide cation (Fig. 5). Tripodal structures derived from pyrazole as tripyridylpyrazolylmethane **3** [81] and their borate analogues **4** [82] form stable and efficient luminescent complexes with Eu^{3+} and Tb^{3+}. With ligands such as **4** the hard lanthanide cations strongly interact with the negatively charged boron and the nitrogenated harms provide good shielding of the metal from the quenching solvent molecules.

A review that describes a huge number of these ligands and the emission properties of their Eu^{3+} and Tb^{3+} complexes has been recently reported [83].

Polydentate ligands based on 2-hydroxyisophthalamide (IAM) **5a**, **6a** and 1-hydroxypyridin-2-one (1,2-HOPO) **5b**, **6b** (Fig. 5) characterized by very high sensitization efficiency towards Eu^{3+} and

Tb^{3+} together with exceptional stability and water solubility have been developed by Raymond and coworkers [84].

A very important class of acyclic ligands is based on polyaminopolycarboxylate systems in which four or more acetic groups are covalently attached to a polyamino skeleton such as ethylendiaminetetraacetic acid EDTA or diethylentriaminepentaacetic acid DTPA that form anionic Ln^{3+} complexes highly stable and soluble in aqueous medium. A huge amount of research has been developed, since many years, on the design and synthesis of substituted DTPA ligands because their Gd^{3+} chelates find application as Magnetic Resonance Imaging (MRI) agents [85]. The currently used Gd^{3+} chelates are based on linear or macrocyclic polyaminopolycarboxylate ligands whose structures, trade names and thermodynamic stabilities are reported in Fig. 6.

It is worth to stress that the stabilities of these Gd^{3+} complexes is so high that the risk of acute toxic effect due to the dissociation of the complex in the living tissues is practically non-existent [86].

Because of the very high stability of Eu^{3+} and Tb^{3+} complexes with DTPA they have been covalently linked to biologically active molecules and have been largely used as label for biological assays by means of Dissociation-Enhanced Lanthanide Fluorescence ImmunoAssay (DELFIA) technique [87]. The covalent insertion into the DTPA structure of appropriate chromophores that can promote the sensitized light emission gives rise to strongly luminescent and stable lanthanide complexes. Ligand as **8** with a carbostyril-124 antenna has been easily prepared starting from the commercially available DTPA bis-anhydride [88].

More symmetric luminescent ligands such as **7** have been prepared by multistep syntheses and the luminescent properties of a number of lanthanide complexes have been investigated [21].

Again Eu^{3+} and Tb^{3+} complexes of **7** and **8** (Fig. 7) show high luminescence quantum yields and long emission lifetimes in aqueous solution being the lanthanide centre perfectly shielded from the environment. Indeed, no water molecules have been found in the first coordination sphere of the complexed metal.

A huge variety of ligands based on pyridine, bipyridine and terpyridine bearing a variable number of acetic groups capable of forming stable complexes with lanthanide cations have been reported by Mukkala research group [89], Fig. 8. In these complexes the polypyridine part of the ligand plays a manifold role, e.g. (i) structural element that determines the topology of the free ligands and of their complexes, (ii) coordination element that provides additional nitrogen binding sites for the lanthanide cation and (iii) sensitization element that, due to its photophysical properties, acts as an effective antenna for the visible light emitting Ln^{3+} complexes. Remarkably, the polypyridine part of the molecule can be functionalized for binding to biologically active compounds thus allowing a wide range of applications in bioanalytical assays [90].

4.6. Macrocyclic and macropolycyclic ligands

A great variety of polyoxa-, polyaza-, and polyoxapolyaza-macrocyclic (coronands) and macrobicyclic (cryptands) compounds have been used as ligands for the preparation of Ln^{3+} complexes. Most of these compounds can be seen as the ring closed version of acyclic polypodands as it is clearly evidenced by structures **9a**,**b** and **10a**–**d**, Fig. 9, where two or three bipyridines of the acyclic **1b** (Fig. 5) are connected to a nitrogen atom through two or three methylene bridges respectively. The bipyridine unit behaves both as binding subunit and as antenna so that **9a**,**b** and

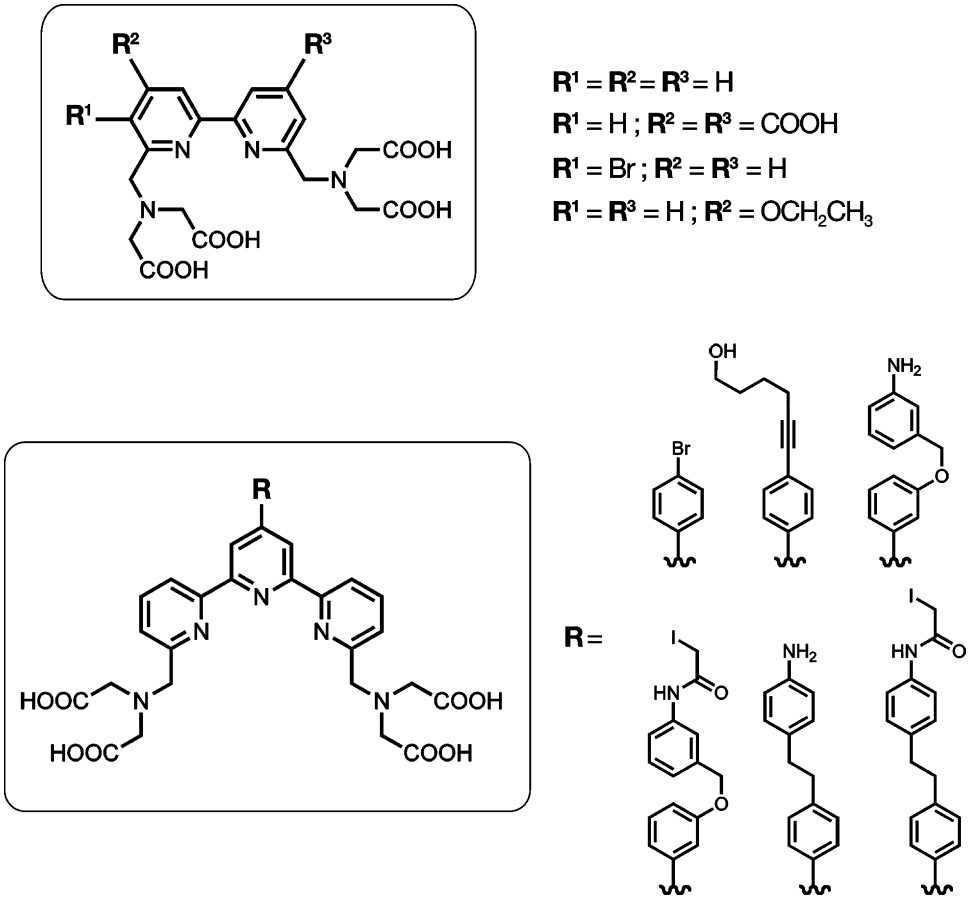

Fig. 8. Examples of pyridine, bipyridine and terpyridine based-ligands used in the preparation of highly stable lanthanide complexes.

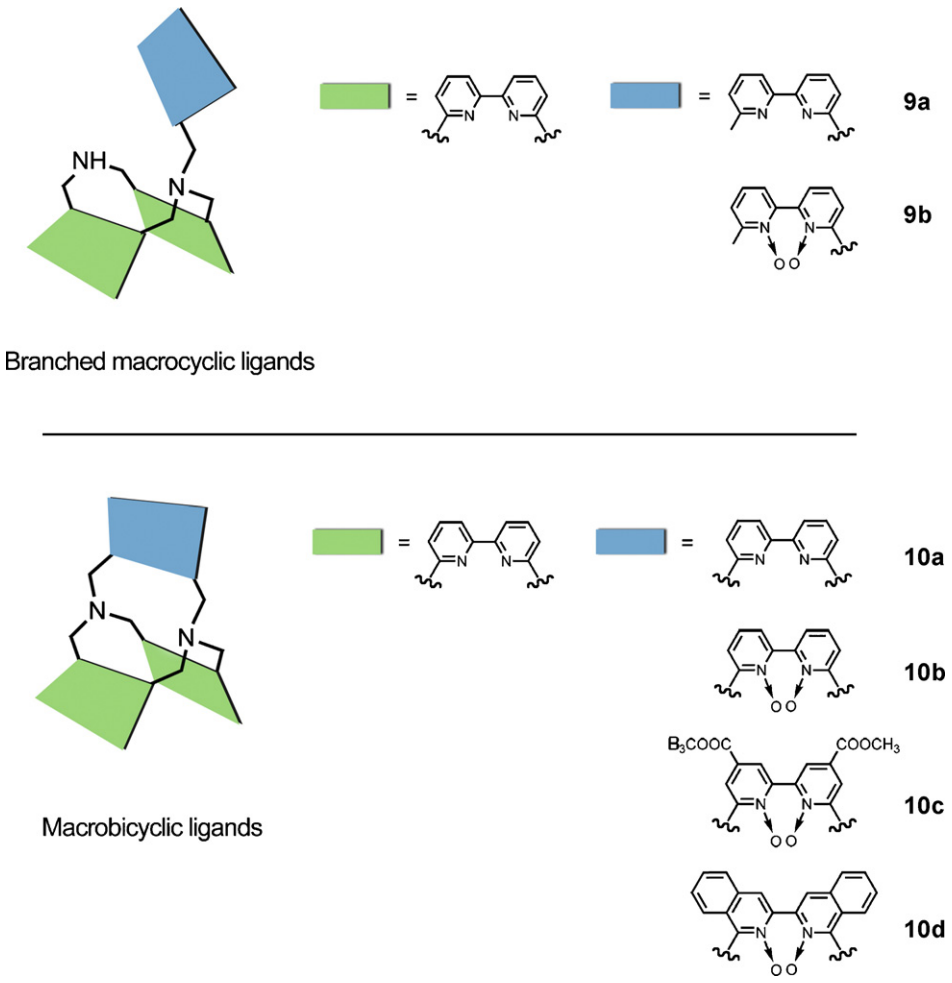

Fig. 9. Examples of N-based cyclic ligands.

10a–d are suitable ligands for the preparation of luminescent Ln^{3+} complexes showing an enhanced kinetic stability because of the increased rigidity of the system on going from ligand **1b** to ligands **9a** and **10a**.

Cryptands are the best candidates for the coordination of spherical alkali and alkali-earth cations [68]. Notably, alkali cryptates show peaks of selectivity due to the complementarity of the size of the metal cation with the dimension of the coordinating cavity ("lock and key" criterion). However the control of the ligand topology based on the latter principle may fail in controlling the stability and selectivity of complexation with Ln^{3+} ions due to the small variation of the cationic radii along the series. Nevertheless interesting macrobicyclic ligands have been synthesized which provide high stability and good energy transfer for the sensitization of Eu^{3+} and Tb^{3+}. In fact $Eu^{3+} \subset$ **10** and $Tb^{3+} \subset$ **10** have been used in Fluorescence Resonance Energy Transfer (FRET) immunoassays [91].

Ligands featuring an intermediate character between the highly preorganized "lock and key" based macropolycyclic and the preorganized "induced fit" systems are also useful with lanthanide ions. Such ligands may contain a polyaza-macrocycle with pendant additional anionic binding sites covalently linked to the secondary amine nitrogen atom of the ring. The stability of the complexes can be tuned by adjusting the ring size and the number and nature of the lateral binding arms that envelope the lanthanide cation. Among all the ligands known, 1,4,7,10-tetraazacyclododecane-1,4,7,10-tetraacetic acid (DOTA, **11**) proved to be the best one for Ln^{3+} with the highest stability constants ever observed ($\log K_{ML}$ in the range 22–29), Fig. 10 [92,93]. The four nitrogens of the cyclen ring bind cooperatively to the face of the square antiprism, corresponding to a widely observed crystal structure for DOTA-type complexes with Ln^{3+} cations, by adopting the same quadrangular conformation either in the free or complexed state [94].

Other aza-macrocycles such as 1,4,7-triazacyclononane (**12**) and 1,4,8,11-tetraazacyclotetradecane (cyclam, **13**) bearing appended acetic groups have been also used; although their Ln^{3+} complexes feature several orders of magnitude lower thermodynamic and kinetic stability constants [88,93]. The introduction of an appropriate number of picolinate and acetic groups on the triazacyclononane ring affords ligands that form lanthanide complexes characterized by high thermodynamic stability and good water solubility, Fig. 10.

Depending on the Ln^{3+} cation, these complexes are interesting either as contrast agents or as luminescent labels for biological assays. For instance, the Tb^{3+} complex **12a** of an octadentate ligand bearing one acetic and two picolinate groups showed $\phi_{se} = 0.43$ in water with a luminescence lifetime $\tau = 1.49$ ms, while only moderate values, $\phi_{se} = 0.05$ and $\tau = 0.54$ ms, have been found for the Eu^{3+} complex under the same conditions. These results indicate that the efficiency of the picolinate group as sensitizer is very high for Tb^{3+} compared to Eu^{3+} [95].

It has been demonstrated that the size of the chelating ring also influences the stability of the complex. Indeed the substitution of one acetate group of DOTA or of DTPA with a propionate residue lowers the stability of Ln^{3+} complexes of at least two orders of magnitude [96].

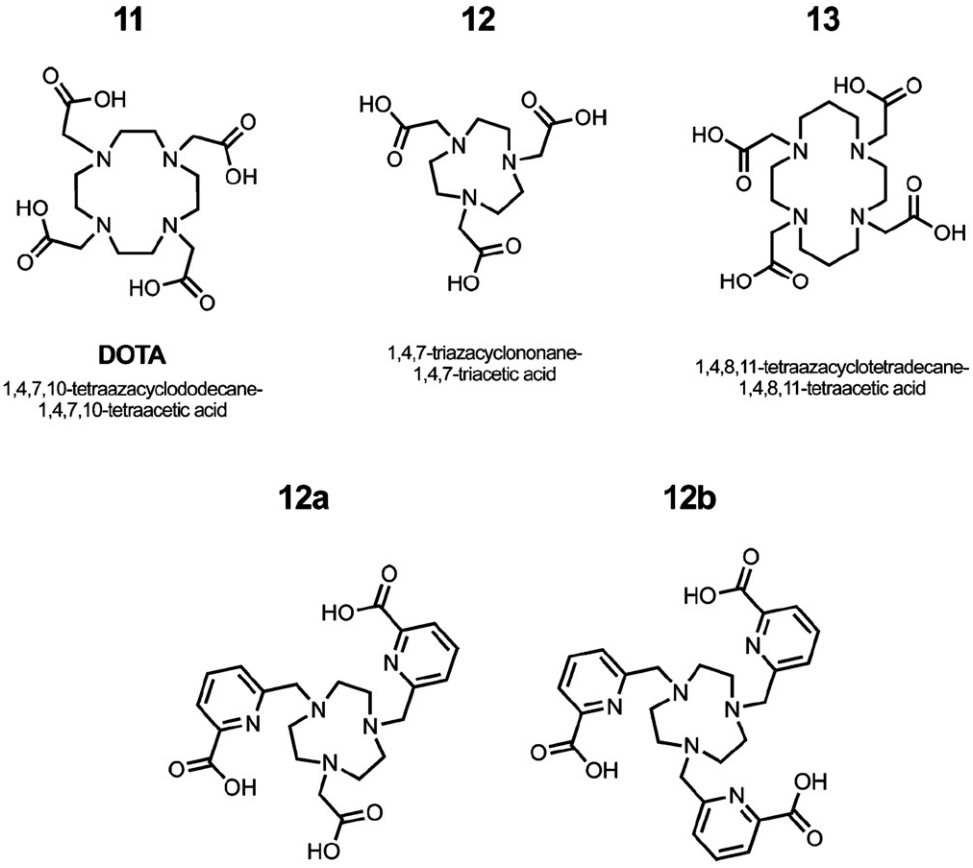

Fig. 10. Examples of polyaza-macrocycle ligands.

4.7. The two-component approach

Our interest in the Ln^{3+} sensitized light emission started several years ago and was aimed at the design and synthesis of Ln^{3+} complexes to be used as new luminescent probes for biological applications. The results of these researches contributed to show that conceptually simple two-component ligand systems can result in remarkable performances in air-equilibrated water sol-

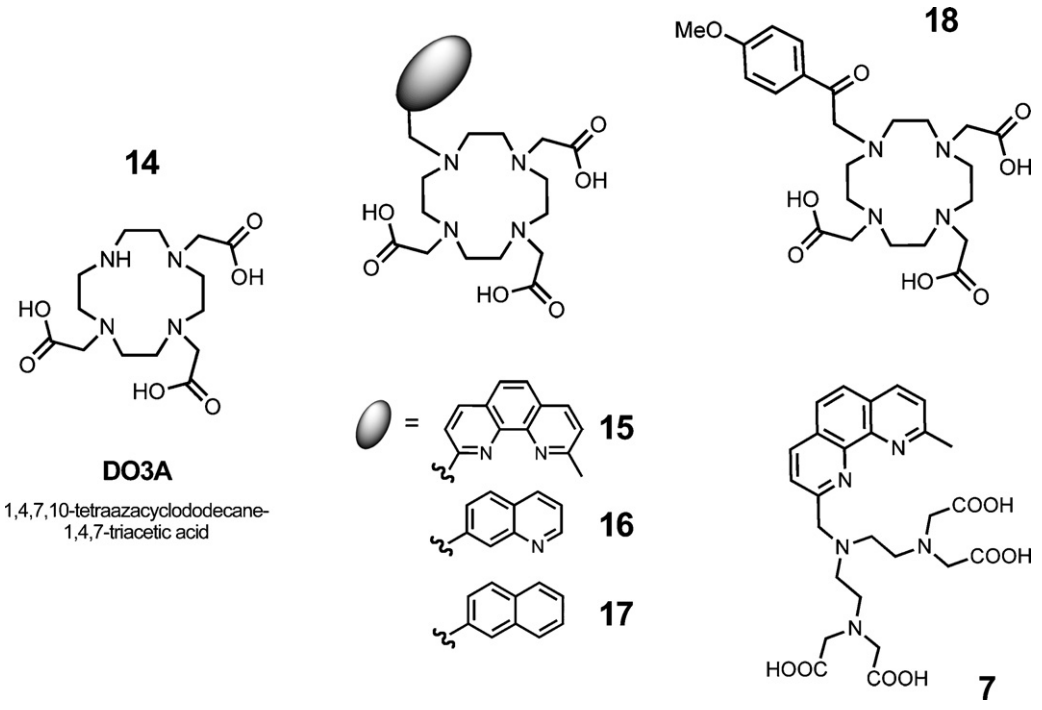

Fig. 11. Examples of ligands containing different types of light harvesting units.

vent [21,22,97,98]. The aspects that we considered in the design of ligand were: (i) high structural simplicity, in the sense that it should contain only the essential elements namely: a good chromophore and an efficient coordination site connected by a short and flexible spacer; (ii) high water solubility; (iii) high chemical and thermal stability; and (iv) easy synthetic accessibility.

In turn, the Ln^{3+}complexes of these ligands should be characterized by: (i) high thermodynamic stability and high kinetic inertness; (ii) good solubility in aqueous medium; (iii) complete shielding of the complexed Ln^{3+} cation in order to minimize the presence of solvent molecules in the first coordination sphere of the metal and hence to reduce the deactivation associated with vibronic coupling; and (iv) high overall sensitization quantum yield.

Following these lines we first synthesized ligands **7** and **15** (Fig. 11). These ligands contain a phenanthroline as the chromophore connected by one methylene to the secondary nitrogen atom of diethylenetriaminetetraacetic (DTTA) and 1,4,7,10-tetraazacyclododecane-1,4,7-triacetic acid (DO3A, **14**) as hosting groups, respectively. Ligands **7** and **15** show nine overall binding sites for the Ln^{3+} cation and it is well known from the literature that DTTA and DO3A form very stable lanthanide complexes in aqueous solution [86].

Of course the removal of one acetic binding site either on DTPA or DOTA plays a negative role on the stability of the complexes but this is partly compensated by the antenna that contains additional binding sites, suitably positioned in order to complete the coordination sphere of Ln^{3+}.

Indeed Eu^{3+} and Tb^{3+} complexes of **15** are highly stable in aqueous solution with the metal centre completely shielded ($q = 0$) from the environment as evidenced by the X-ray crystal structure of the $Eu^{3+} \subset$ **15** and solution structural investigation by ^{1}H NMR.

In Fig. 12 are reported the X-ray crystal structures of $Eu^{3+} \subset$ **15** and $Er^{3+} \subset$ **15** complexes. The two structures are isomorphous and, in both cases, the metal cation is nonacoordinated by the four nitrogen atoms of the macrocycle, the three carboxylic groups and the two nitrogen atoms of the phenanthroline and, as already pointed out, there are no water molecules coordinated to the metal cation. It is interesting to point out that because of coordination the phenanthroline moiety is strongly distorted from planarity. By considering the least square plane of the central ring the greater deviations are observed for the atoms C24 and C25 from one side of the ring and for the atom C17 from the other side. They are placed at 0.570, 0.495 and 0.395 Å from this plane respectively for the europium complex. Slightly higher values have been observed for the Er^{3+} complex [97].

The presence of binding sites properly positioned on the chromophore is an important requisite for the luminescence efficiency of the Ln^{3+}complexes. Thus, Eu^{3+} and Tb^{3+} complexes of ligands **16** and **17** (Fig. 11) having a quinoline or a naphthyl group as antenna showed lower sensitization quantum yields. Indeed the quinoline group contains one nitrogen atom as a potential binding site that is however unsuitably positioned to effectively coordinate the metal. As a consequence water molecules ($q = 1.5$) are present within the coordination sphere of the metal [98].

Another interesting ligand, reported by Beeby et al. [35] and conceptually similar to **15**, is compound **18** (Fig. 11) that bears an acetophenone residue as antenna. In this case also the carbonyl group coordinates the metal centre and the coordination sphere of the metal is completed by one molecule of water ($q = 1$). The overall sensitization efficiencies found for $Eu^{3+} \subset$ **18** and $Tb^{3+} \subset$ **18** in aqueous solution are $\phi_{se} = 0.096$ and 0.34 respectively.

4.8. *Photophysical properties of Ln^{3+} complexes of model systems **15** and **7***

System **15** features the combination of a phenanthroline (phen) as the light antenna and a tetraazacyclododecane–triacetic acid unit, DO3A, as the hosting unit for the cation. DO3A provides seven binding sites for coordination of the Ln^{3+} cations, and the 1:1 DO3A:Ln^{3+} association constant is remarkably high, $\log K_{ML} = 23$

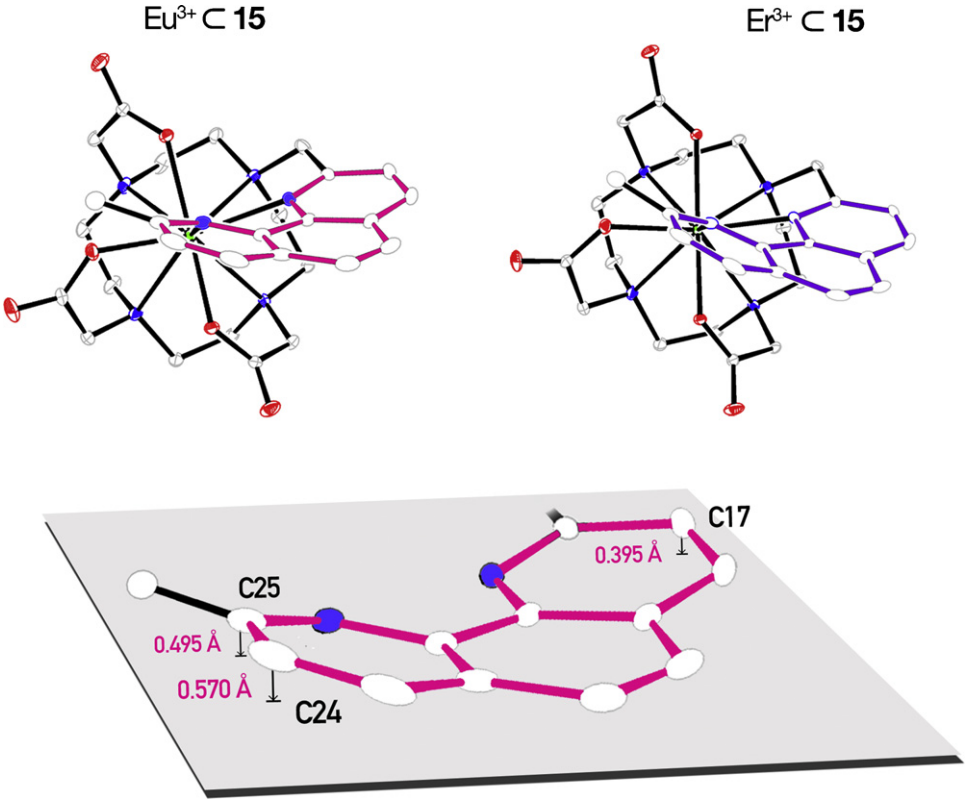

Fig. 12. X-ray structures of $Eu^{3+} \subset$ **15** and $Er^{3+} \subset$ **15**.

Table 2
Metal centred luminescence properties for Ln^{3+} complexes of systems **15** and **7** in H_2O and D_2O solutions[a].

	H_2O					D_2O	
	λ_{max}[b] (nm)	ϕ_{se}	τ (μs)	k_r (s^{-1})	k_{nr} (s^{-1})	ϕ_{se}	τ (μs)
$Eu^{3+} \subset$ **15**		0.21	1240	169	637		1770
$Tb^{3+} \subset$ **15**		0.11	310	355	3020		320
		0.55[c]	1510[c]	364[c]	298[c]		
$Eu^{3+} \subset$ **7**	616	0.24	1250			0.30	1880
$Tb^{3+} \subset$ **7**	544	0.15	780			0.14	820
		0.45[c]	2.3×10^{3}[c]				
$Sm^{3+} \subset$ **7**	598	2.5×10^{-3}	13.0			2.5×10^{-3}	34.0
$Dy^{3+} \subset$ **7**	478	5×10^{-4}	1.2			5×10^{-4}	1.1

[a]At room temperature, excitation at 278/279 nm; for Sm^{3+} and Dy^{3+} complexes, results are for the Vis emission portion; no water molecules (q) are present in the coordination sphere of the Ln^{3+} centre, uncertainty on q is ±0.5 [21,22,97]. [b]Highest intensity band. [c]Degassed samples.

[92,93]. The use of phen as a light absorbing unit allows to set up an efficient antenna–lanthanide system because: (i) the ISC step for phen takes place with $\phi_{ISC} \approx 0.65$ (presumably, not far from unit) within the complex; (ii) the rate constant for the energy transfer step is $k_{en} \approx 10^7\ s^{-1}$, which compared to a deactivation rate constant $k_T \sim 3 \times 10^4\ s^{-1}$ for the phen T level (Fig. 2) results in $\phi_{en} \sim 1$; and (iii) the phen moiety cooperates to saturate the coordination sphere around the cation so that no water molecules are directly bound to the Ln^{3+} centre, $q = 0$, (Eq. (2a)). A similar approach led to the $Eu^{3+} \subset$ **18** system where the single chromophore playing as an antenna was acetophenone, and q^{Eu} was found to be 1. Table 2 lists some the luminescence results obtained in water solution with system **15**.

Good performances were likewise obtained with the water-soluble ligand **7** which is constituted by a single phen chromophore and a diethylenetriamine tetraacetic unit (DTTA) hosting site that, as expected, provides thermodynamically stable and kinetically inert complexes. The coordination positions of the Ln^{3+} centre are protected against solvent access, as shown by the comparison of luminescence results obtained in water and deuterated water, Table 2. We provided evidence that for the 1:1 species obtained with ligand **7** ($\log K_A > 7$), the luminescence sensitization process in air-equilibrated water is quite effective, resulting in $\phi_{se} = 0.24$ and 0.15 for the visible emitters $Eu^{3+} \subset$ **7** and $Tb^{3+} \subset$ **7**, respectively and $\phi_{se} = 2.5 \times 10^{-3}$ and 5×10^{-4} for the visible portion of the $Sm^{3+} \subset$ **7** and $Dy^{3+} \subset$ **7** emitters, respectively [21]. In the following, for the sake of illustration we discuss some issues concerned with the spectroscopic properties of the complexes obtained with ligand **7**.

4.9. Absorption and emission properties

Representative absorption spectra of **7** and $Eu^{3+} \subset$ **7** in water solution are shown in Fig. 13 together with the results from luminescence titration of **7** upon $EuCl_3(H_2O)_6$ addition. Results of the titration experiment illustrated in insets (a) and (b) of Fig. 13 indicate that a 1:1 association takes place, with an evaluated association constant $\log K_{ML} > 7$ [97].

The absorption spectra of **7** and $Eu^{3+} \subset$ **7** show a high degree of overlap with the two peaks in the UV region at 230 and 279 nm being ascribed to ligand-centred transition of the phenantroline group; similar results were obtained for other $Ln^{3+} \subset$ **7** complexes. The fact that the absorption profiles of **7** and $Eu^{3+} \subset$ **7** are identical is not a common observation because the triply charged ion incorporated within a complex usually affects the electronic properties of the nearby chromophore, in turn resulting in a change of its absorption profile. Thus, for the case of **7**, it seems that coordination of the phen unit at the Ln^{3+} centre does not actually imply a strong electronic interaction between these two units. Nevertheless, efficient sensitization of the MC luminescence takes place, as revealed both by the titration course in Fig. 13 and by the final intense luminescence observed for $Eu^{3+} \subset$ **7**, Table 2. In conclusion, the weak electronic interaction between the light absorbing phen of **7** and the light emitting Ln^{3+} subunits appears large enough to promote the occurrence of ligand-to-metal energy transfer. A similar case from the literature was that of a $Eu^{3+} \subset$ **18** system with appended a single acetophenone unit [35].

4.10. Ligand-centred luminescence

According to Fig. 2 and to the results described above for $Eu^{3+} \subset$ **7**, light absorption *via* ligand-centred ^{1}LC transitions is followed by an intersystem crossing step (ISC), leading to population of the lowest-lying triplet level (T) of phen origin. The observed lanthanide luminescence originates from subsequent ligand-to-metal intramolecular photoinduced energy transfer processes. Fig. 14 shows the luminescence spectra of $Eu^{3+} \subset$ **7**, $Tb^{3+} \subset$ **7**, $Sm^{3+} \subset$ **7** and $Dy^{3+} \subset$ **7**, as registered upon excitation at 279 nm.

As expected, this reference scheme does not work for the case of Gd^{3+} complexes because its lowest-lying MC level is located at 32,150 cm^{-1} (corresponding to the $^6P_{7/2} \rightarrow {}^8S_{7/2}$ transition), an energy content much higher than that of the T level of most organic chromophores. On this basis, the luminescence study of $Gd^{3+} \subset$ **7** allows to evaluate the energy levels of the lowest-lying singlet (S) and triplet (T) excited states of the chromophore, as affected by a nearby heavy and triply charged center. Fig. 15 shows the luminescence results for **7** and $Gd^{3+} \subset$ **7** as obtained at room tem-

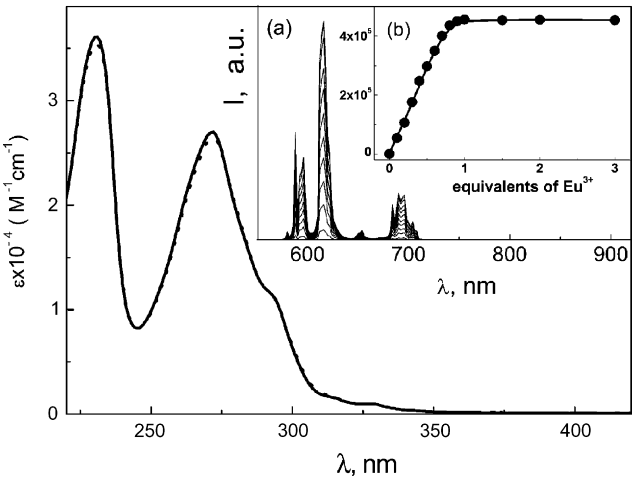

Fig. 13. Titration experiment of water solution of 7 upon $EuCl_3(H_2O)_6$ addition. Shown are (i) the absorption spectra of **7** (full line) and $Eu^{3+} \subset$ **7** (taken at the end of the experiment, dotted line), (ii) the enhancement of the metal centred luminescence, $\lambda_{exc} = 279$ nm, upon addition of Eu^{3+}, inset (a), (iii) the registered changes of the emission intensity at 616 nm (filled points) and the full line resulting from the fit of the data points according to a 1:1 stoichiometry, inset (b) Ref. [21].

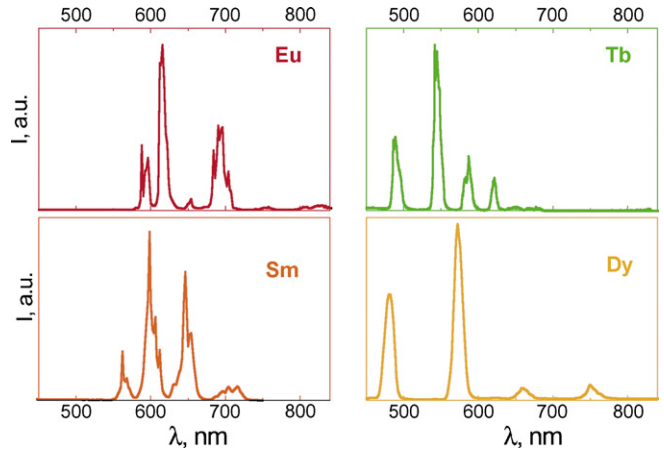

Fig. 14. Room temperature emission spectra in the Vis portion for the $Ln^{3+} \subset$ **7** complexes of the indicated cations; in air-equilibrated D_2O, λ_{exc} = 279 nm. For $Sm^{3+} \subset$ **7** and $Dy^{3+} \subset$ **7**, in the NIR portion of the emission (not shown), the luminescence profile exhibits a maximum intensity peak at 948 and 994 nm, respectively.

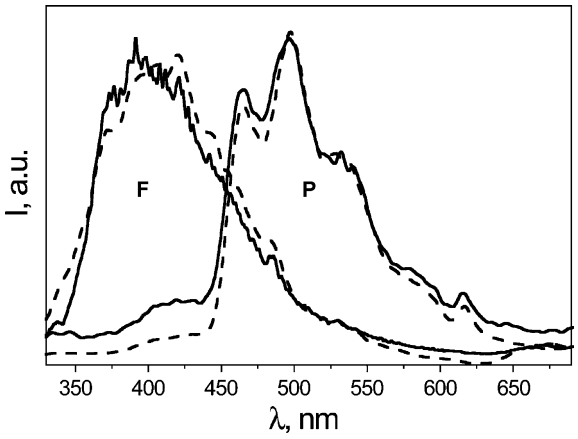

Fig. 15. Fluorescence (F, room temperature) and phosphorescence (P, 77 K, pulsed lamp, 10 ms delay after flash) spectra of **7** (solid line) and $Gd^{3+} \subset$ **7** (dashed line) in water solution and rigid matrix; λ_{exc} = 279 nm.

perature (fluorescence) and at 77 K (phosphorescence) and Table 3 lists luminescence data for the ligand-centred emission at both temperatures.

With regard to the room temperature results as monitored at the fluorescence band for **7** ($\phi_{em} = 3.5 \times 10^{-3}$ and τ = 0.9 ns) and for $Gd^{3+} \subset$ **7** ($\phi_{em} = 7.4 \times 10^{-4}$ and τ < 0.5 ns), one draws the indication that the metal centre causes an improved intersystem crossing within the complex. As for the 77 K results, from the highest energy peak of the phosphorescence profile, the T level of phenanthroline origin can be estimated to lay at 22,100 cm^{-1} for both **7** and $Gd^{3+} \subset$ **7**, a result consistent with findings from previous investigations [51]. As seen above, Fig. 2 compares typical energetic layouts for the cases of Tb^{3+}, Eu^{3+}, and Gd^{3+}, with highest-energy transitions labeled $^5D_4 \rightarrow {}^7F_6$, $^5D_1 \rightarrow {}^7F_0$, and $^6P_{7/2} \rightarrow {}^8S_{7/2}$, respectively.

Table 3
Ligand-centred luminescence properties for **7** and $Gd^{3+} \subset$ **7** in H_2O solution and rigid matrix[a].

	298 K			77 K	
	λ_{max} (nm)	ϕ_{em}	τ (ns)	λ_{max} (nm)	τ (s)
7	370	3.5×10^{-3}	0.9	498	1.7
$Gd^{3+} \subset$ **7**	380	7.4×10^{-4}	<0.5	498	0.23

[a] Fluorescence at room temperature and phosphorescence at 77 K (frozen medium) of **7**; λ_{exc} = 279 nm.

4.11. Coordination features

$Eu^{3+} \subset$ **7** and $Tb^{3+} \subset$ **7** show a remarkably intense and long-lived luminescence in both H_2O and D_2O solutions (Table 2). Comparison of luminescence results for water and deuterated water provides an assessment of water binding at the Eu^{3+} and Tb^{3+} centres, (Eq. (2)). In particular, for $Eu^{3+} \subset$ **7** and $Tb^{3+} \subset$ **7** we found q^{Eu} = 0.02 and q^{Tb} = 0.01, respectively [21]. These results clearly indicate that the coordination shell of system **7** effectively prevents water from binding at the metal centres so that the OH oscillators are kept far from the metal centres and cannot act as quenchers. Similarly, for $Sm^{3+} \subset$ **7** and $Dy^{3+} \subset$ **7** no solvent molecules (q = 0) were thought to be present within the first coordination sphere.

4.12. Oxygen effect

Comparison of luminescence intensity and lifetime data in air-equilibrated and degassed water solutions reveals an oxygen effect for the $Tb^{3+} \subset$ **7** case, Table 2. This effect is due to a small energy gap, ΔE, between the T ligand-centred and MC levels, Fig. 2. Because of thermal redistribution, both forward (ligand-to-metal) and backward (metal-to-ligand) energy transfer processes take place, with rate constants, k_f and k_b, respectively. This allows the non-radiative deactivation of the T level of the ligand *via* a triplet–singlet electron exchange energy transfer process, which is possible because of the overlapping between the excited T state of the ligand and the ground state vibrational levels of the oxygen molecules (see Fig. 2). For all the complexes but those of Tb^{3+}, no changes of luminescence properties were observed for air-equilibrated and degassed samples (Table 2). A distinctive reason for the lack of oxygen effect is met for the case of $Dy^{3+} \subset$ **7**. The highest-energy level of Dy^{3+} is at ~20,750 cm^{-1} (corresponding to the $^4F_{9/2} \rightarrow {}^6H_{15/2}$ transition) and is close-lying to that of Tb^{3+}, ~20,500 cm^{-1} ($^5D_4 \rightarrow {}^7F_6$). In contrast with the $Tb^{3+} \subset$ **7** case, the faster luminescence decay of $Dy^{3+} \subset$ **7** (1.2 μs, Table 2) forbids the establishment of an equilibrium between the ligand (T) and Dy^{3+} centred levels (that decreases the rate of the energy transfer process making it competitive with the oxygen effect), thus preventing the luminescence quenching by O_2.

4.13. Nature of the energy transfer step

As seen above, efficient phen → Ln^{3+} energy transfer takes place for the complexes of Table 2. On this basis, it can be concluded that $\phi_{ISC} \times \phi_{en} \approx 1$ [from Eq. (1), oxygen-free case for Tb^{3+} complexes]. This result is consistent with those from ^1H NMR spectroscopy, suggesting the involvement of the phen subunit in the coordination of the metal cation [22]. Concerning the non-radiative energy transfer processes, Förster [72] and Dexter [73] have proposed two different mechanisms involving coulombic and exchange interactions, respectively. The former (Förster-type), dominated by long-range dipole–dipole interactions, does not require physical contact between the interacting partners; it is sufficient that the excited sensitizer induces a dipole oscillation on the acceptor (A) center. As a consequence, it can take place at large intermolecular distance (up to the order of 100 Å). By contrast, electron exchange energy transfer (Dexter-type) requires closer contact between donor (D) and acceptor centers. In fact, the way the energy is transferred can be visualized by a double electron substitution process in which the excited electron on D* (donor center in an excited state) travels to A, whereas one electron on A goes to D. This type of interaction is effective only when the two units are close enough to allow overlap between their electronic charge distributions, i.e. in the presence of physical contact between the sensitizer and the accepting unit. A dipole–dipole through-space (Förster-type) mechanism for energy transfer seems unlikely, given that the energy transfer step involves in all cases a triplet level for the donat-

ing chromophore, a phen subunit for many of the cases examined here. On the other hand, it is known that a very small electronic interaction, i.e. an interaction term $H \sim 1\ cm^{-1}$, is enough to permit the occurrence of Dexter-type through-bond energy transfer [99]. This interaction might originate *via* mediation by the intervening short sequence of bonds separating the phen chromophore and the hosting site for the Ln^{3+} centres.

4.14. Metal centred luminescence

The Eu^{3+} and Tb^{3+} complexes are the most intense emitters among those of the lanthanide series, as shown for the representative cases collected in Table 2. It is interesting to examine the influence of radiative and non-radiative processes in these luminophores. In Table 2, values for the k_r and k_{nr} rate constants, Eq. (1b), are listed as obtained from the observed photophysical parameters and available literature sources. Estimates of the pure radiative lifetime ($\tau_r = 1/k_r$) can be obtained for Eu^{3+} complexes according to an approach which compares the intensity of the $^5D_0 \rightarrow {}^7F_1$ band (593 nm, insensitive to the coordination environment) with the overall shape of the emission spectrum, (Eq. (3)) [21]

$$k_r = A(0,1)\frac{I_{tot}}{I(0,1)} \quad (3)$$

In this equation, $A(0,1)$ is the spontaneous emission probability of the $^5D_0 \rightarrow {}^7F_1$ transition, that is evaluated $32.4\ s^{-1}$ in water [35,100], and $I_{tot}/I(0,1)$ is the ratio of the total integrated intensity of the emission spectrum to the portion of the profile for the $^5D_0 \rightarrow {}^7F_1$ band. Thus, for the Eu^{3+} complexes evaluated values for k_r are in the range $160–240\ s^{-1}$ and those for k_{nr} are even larger (Table 2). On the basis of Eq. (1b), one draws the conclusion that even for the Eu^{3+} complexes, the most luminescent ones within the lanthanide series, the intrinsic efficiency ϕ_{lum}^{MC} cannot reach unity.

To notice that MC non-radiative processes can include both intrinsic and back energy transfer contributions, $k_{nr} = k_{nr}^{MC} + k_b$. The former are related to the presence of OH oscillators, and are therefore depressed in D_2O as pointed out for the Eu^{3+} cases of Table 2. For Tb^{3+} complexes, the energy gap ΔE between the ligand T level and the emissive MC level is usually so small that $Tb^{3+} \rightarrow L$ back energy transfer is by far the major contribution to the non-radiative deactivation, as noticed above for the cases of air-equilibrated water solution. In conclusion, also for the Tb^{3+} complexes, the intrinsic luminescence quantum yield is expected to be lower than unity.

5. Sol–gel techniques for the preparation of photoemissive materials

The peculiar luminescence properties of the lanthanide antenna complexes properly coupled with suitable inorganic or polymeric matrices can be exploited for a variety of modern applications [7,17,63,101–103] ranging from diagnostic tools in nanobiomedicine to optical and photonic materials for the development of lasers, displays and lighting devices, just to cite a few.

The possibility to combine in one material the properties of inorganic or polymeric components with complex organic or organometallic units, such as chromophores, catalytically active groups or biomolecules, has witnessed important improvements in recent years with the development of low-temperature *soft* chemistry solution processes [102–106]. Among them, *sol–gel* and hydrothermal synthesis methods have allowed the preparation of original nanosystems and nanocomposite structures with sophisticated shapes and intriguing peculiarities. The notion is to create materials with new combinations of properties by integrating inorganic or organic components at nanoscale or molecular level. Nowadays, the incorporation of luminescent lanthanide complexes in solid matrices with controlled structural organization is of widespread interest in materials science as it affords functional materials with a variety of optical properties.

Due to the number of scientific publications in this field, this work is far from providing an exhaustive review on the previously performed research activities. For a more detailed discussion on these methodologies, the reader can refer to specific pertinent literature. In this framework exhaustive reviews on different strategies towards lanthanide-doped hybrid materials [106] and Ln^{3+}-containing siloxane-based hybrid materials [102] have been recently reported in the literature.

In the areas of life science, biotechnology and clinical diagnostics, luminescent lanthanide chelates are receiving increasing attention because of their applications as luminescent probes for highly sensitive time resolved fluoroimmunoassay (TR-FIA), DNA hybridization assay, fluorescence microscopy bioimaging, and other analytical techniques [84,90,107–112]. They display specific luminescence properties that conventional organic dyes do not show, such as sharp emission profiles, large Stokes shifts and long luminescence lifetimes (ms scale). Indeed a typical fluorescence bioassay drawback is that the fluorescence detection is easily affected by the background noise (emission lifetime ≈ ns to a few μs) caused by biological samples and analysis instruments [113,114]. By using luminescent lanthanide complexes non specific background fluorescence from the specimen and cuvette materials and the scattering light can be effectively eliminated due to the very long fluorescence lifetime, usually of several hundreds of microseconds. For practical uses, these bio-labelling reagents should be conveniently grafted on suitable substrates, such as inorganic or polymeric nanoparticles (NPs) or colloids [113]. Currently, silica-based NPs are used in many areas of bioanalysis and, compared with polymer-based NPs, they have a reduced tendency to aggregation and toward dye leakage [115,116]. In addition, the silica surface makes these NPs chemically inert and physically stable [117]. All these properties make silica NPs excellent labeling

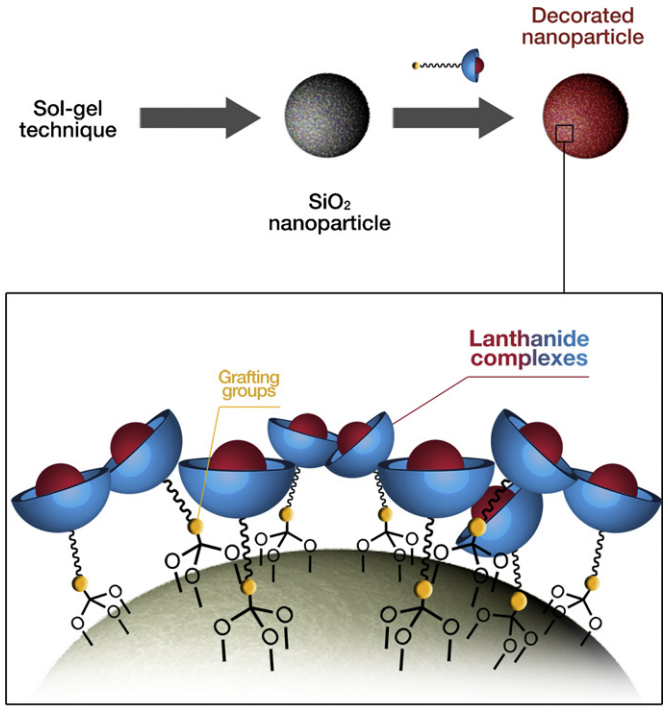

Fig. 16. Schematic representation of a SiO_2 nanoparticle functionalized with luminescent metal complexes.

reagents for bioanalysis and bioimaging [115,118,119]. Through sol–gel synthesis, a single silica particle can be functionalized with a large number of dye molecules, up to tens of thousands, Fig. 16.

Even though luminescence quenching phenomena within the NPs are not completely eliminated, thanks to the large amount of dye incorporated in a small volume, the goal of obtaining nanoparticles with brighter luminescence is achieved. Thus, the main advantage of luminophore-doped NPs concerns the capability to originate highly amplified optical signals compared with a single dye molecule. Moreover, as the dye is protected by the silica matrix, both photobleaching and photodegradation phenomena that often affect conventional dyes can be minimized [120]. Furthermore, thanks to the flexibility of silica chemistry, different types of functional groups can be easily introduced on the NPs surface and, besides single-dye doping, multiple-dye incorporation into the silica matrix is also possible. This can provide more information upon detection. In fact, by tuning the concentrations of the different luminophores within the NPs, excitation with a single wavelength leads to different emission, thus permitting simultaneous and sensitive detection of multiple targets.

Concerning the field of optical materials, lanthanide antenna complexes are being intensively studied, among others, for the development of sensors [67], light-conversion molecular-devices, optical fiber lasers and amplifiers [33,121], and electroluminescent materials [122]. For most applications, such as tunable solid-state laser or phosphor devices, mechanical strength and chemical stability under variable temperature or moisture conditions are severe requisites. Recently, lanthanide hybrid materials obtained by incorporation of lanthanide complexes in the inorganic matrices have attracted considerable interest, and their luminescence properties have been extensively studied. The main goal of these studies was to understand how the photophysical properties of the emissive species can be affected by the interaction with the *host* structure [102,106,123]. Consequently, considerable research activity is being carried out to improve the chemical stability and to adapt the materials chemistry to the production technology of the concerned application. Depending on the chemical nature of the components, materials characterized only by weak interactions between organic and inorganic parts (such as hydrogen bonding, Van der Waals forces, or electrostatic forces) can be obtained [102,106,123–125]. However inhomogeneous dispersion of two phases and leaching of the photoactive molecules frequently occur; in these cases the allowed concentration of complex is also severely restricted. Alternatively, an appealing possibility is the covalent bonding of rare-earth antenna complexes to the *host* network [126,127] through *soft sol–gel* chemistry. The tuning of the interactions between the luminescent species and the *host* medium represents a fundamental aspect [128]. Indeed, the properties that can be obtained for such materials certainly depend on the chemical nature of their components and on their molecular level structure. *Sol–gel* chemistry allows the combination at the nanoscale level of inorganic and organic components in a single hybrid composite [104], opening thus access to an expanding area of innovative materials and to new perspectives in materials science [102,106,123,129–133]; moreover, a prominent advantage of the technique is that the microstructure and shape can be controlled by varying the sol–gel processing conditions. The use of the sol–gel technique for the synthesis of oxide-based materials [134,135] is thus attracting much attention. In particular, in the design of luminescent hybrid materials based on lanthanide antenna complexes, due to its chemical stability and transparency, silicon dioxide (SiO_2, *silica*) is suitable as *host* material either for the development of optical materials or as a substrate in biotechnology and clinical diagnostic. The chemistry of the sol–gel process is mainly based on hydrolysis and polycondensation of metal alkoxides to form extended networks with an oxide skeleton. Although the utility of sol–gel matrices as *hosts* for organic and organometallic components has been well known since long, it still attracts increased attention in basic research for designing appropriate sol compo-

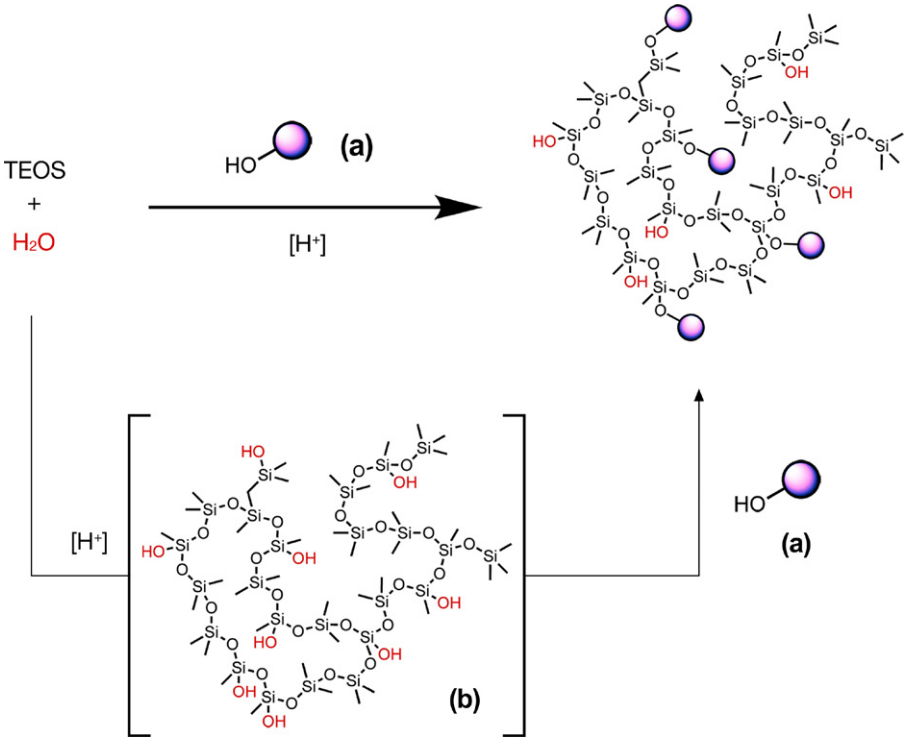

Fig. 17. Schematic representation of chemical grafting of functional complexes in a sol–gel silica matrix.

Table 4
Room temperature luminescence data in solution and in the silica films (Ln/Si = 1/400).

	H_2O[a] ([Eu] = [Tb] = 10^{-5} M)		D_2O[a] ([Eu] = [Tb] = 10^{-5} M)		SiO_2 matrix[a,g]	
	ϕ_{se}	τ (ms)	ϕ_{se}[b]	τ (ms)	ϕ_{se}[b]	τ (ms)
$Eu^{3+} \subset$ **19**	0.18	1.25	0.31	1.82	0.25	1.2
$Tb^{3+} \subset$ **19**	<0.001[c]	[d]	<0.001	[d]	<0.001	[d]
$Eu^{3+} \subset$ **15**	0.21[e]	1.24[e]	0.30[f]	1.77[f]	0.19	1.25
$Tb^{3+} \subset$ **15**	0.11[e] (0.55)[e]	0.31[e] (1.51)[e]	0.12	0.32	0.15	1.1
$Eu^{3+} \subset$ **18**	0.07	0.6	0.25	2.2	0.12	0.7
$Tb^{3+} \subset$ **18**	0.34	1.7	0.54	2.5	0.45	1.5
$Eu^{3+} \subset$ **20**	0.08	0.6	–	–	0.08	0.6
Eu_2–Tb_1	–	–	–	–	–	–
Eu_1–Tb_1	0.19	0.7[h] 1.7[i]	–	–	0.19	0.7[h] 1.7[i]
Eu_1–Tb_2	–	–	–	–	–	–
$Tb^{3+} \subset$ **20**	0.31	1.6	–	–	0.31	1.6

[a] $\lambda_{exc} = \lambda_{max}$; [b] average values obtained with three measurements. [c] Negligible improvements have been recorded by removing oxygen upon bubbling with argon for 10 min; [d] not reported due to the weakness of the signal. [e] From Ref. [97]. [f] From Ref. [22]. [g] A 450 W Xe lamp was used as light source for the excitation of the glassy samples. The use of laser as an excitation source to measure the thin films (tens of nm) quantum yield may result unsuitable because the high energy power and the reduced size of the spot generate a partial deterioration of the sample during the measurement, leading to a subestimation of the emission efficiency. On the contrary, less energetic arc lamps (i.e. Xe lamp) avoid such problem. In brackets () = degassed sample. [h] Eu^{3+}-centred emission. [i] Tb^{3+}-centred emission.

sitions for development of *host* matrices for functional molecules such as lanthanide antenna complexes (*guests*). The luminophores, (a) in Fig. 17, can be anchored to the silica *host* through –OH groups during glass synthesis, thus yielding highly homogeneous materials with covalently linked complexes (Fig. 17). Actually, the grafting of the *guest* molecules in/on the *hosting* phase is performed through a *one-step* process favoured by the intimate mixing of molecular reactants in the starting solution. This allows, in principle, a fine control over luminophore dispersion and avoids undesired aggregation phenomena. Alternatively, the functionalization of sol–gel materials can be performed as a *post-synthesis* step, by exploiting the presence of residual –OH groups, (b) in Fig. 17, that can provide reaction sites for chemical grafting of different species [136,137] and whose amount can be tailored depending on processing conditions.

For the covalent insertion of antenna complexes within the chosen matrix, the presence of suitable grafting groups in the chromophores represents a mandatory requisite. A proper site for functional groups (e.g. hydroxyl, amino groups, etc.) in the complexes is usually represented by the antenna unit. Hence, covalent linking results convenient if simple synthetic procedures to functionalize the emitting compounds are readily available. Alternatively, the possibility to stably embed different chromophores in the same oxide matrix while keeping unaltered their emission behaviour represents a real advantage and performing light-emitting devices can be prepared with wide flexibility.

To this respect, we have recently explored the possibility to rationalize the chemical design of emissive materials based on the embedding of luminescent molecular components into transparent oxide layers. In particular, we have considered two aspects on the photoluminescence performances of the final materials: (i) the nature of the antenna (acetophenone *vs.* phenanthroline derivatives) and coordination features at the Ln cations, i.e. the energy of the sensitizer triplet states (see above), that affects the efficiency of energy transfer to the Ln^{3+} emitting states, and (ii) the role played by the nature of the chromophore incorporation, i.e. covalent linking *vs.* blending of the emissive components in the *host* matrix.

Following simple fabrication procedures, we have grafted by sol–gel different lanthanide antenna emitters to silica glassy layers in controlled combination thus gaining relevant ready colour tunabilities. This is a key aspect especially in the lighting industry, where light-emitting devices and displays comprising rare-earth complexes embedded into an inorganic network are of growing interest, especially in the form of thin layers. Among Ln elements, Eu^{3+} and Tb^{3+} feature exclusive luminescence and well-known properties as red ($\lambda_{em}^{max} = 614$ nm) and green ($\lambda_{em}^{max} = 544$ nm) emitters. In the last years, we have explored the possibility to synthesize highly luminescent films through incorporation of various Eu(III) and Tb(III) complexes in SiO_2 glassy films via sol–gel, using $Si(OC_2H_5)_4$ (TEOS) as the silica source and following a well established procedure [126,127].

In a study [127,138], Eu(III) and Tb(III) antenna complexes employing different units – phenanthroline and acetophenone derivatives – for light absorption and sensitization of the lanthanide (Ln) emitting states, were synthesized and successively anchored in the silica layers. Irrespective of the employed antenna, of covalent linking or blending of the emissive components (*host–guest*

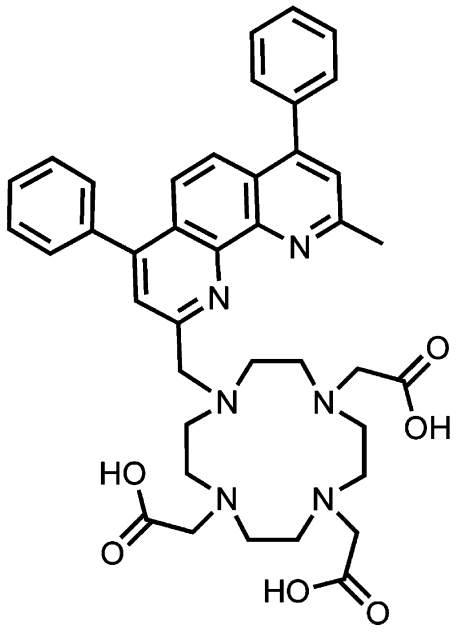

19

Fig. 18. Macrocyclic ligand functionalized with a bathocuproine group as light harvesting unit.

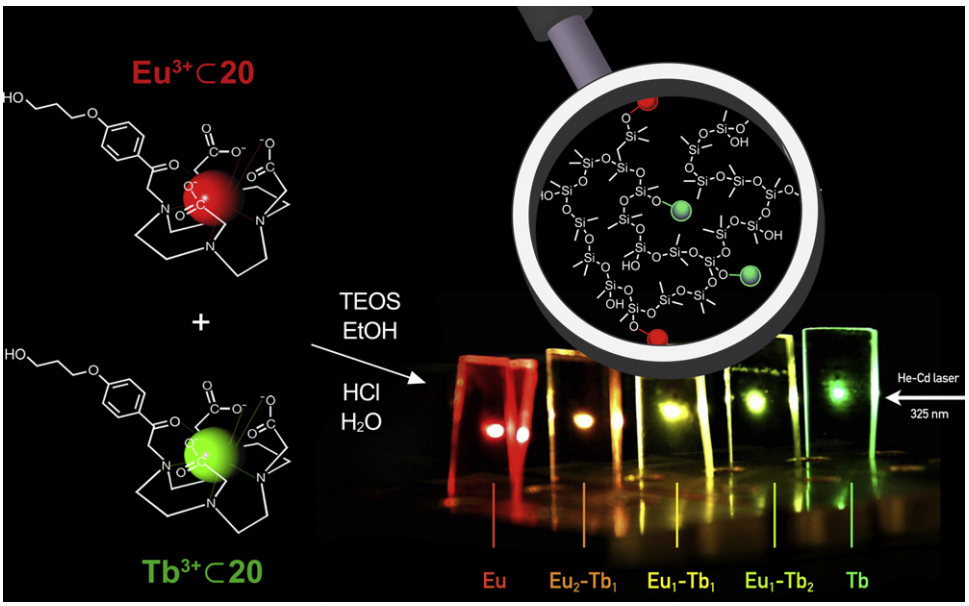

Fig. 19. Colors emitted by silica layers containing different ratios of $Eu^{3+} \subset$ **20** and $Tb^{3+} \subset$ **20** complexes.

interactions), and of antenna complexes concentration in the films, as-deposited layers resulted homogeneous, well-adherent to the substrates, transparent and crack free. Moreover, the macroscopic appearance of the specimen was not affected by the densification thermal treatment, up to 200 °C for 5 h. In the silica layers, Ln^{3+} complexes showed remarkable luminescence intensities, with quantum yields up to 45% for $Tb^{3+} \subset$ **18** (see Table 4); an exception was observed for $Tb^{3+} \subset$ **19** (Fig. 18), in which the sensitization process is not successful because of the unfavorable energy gap between its donor (bathocuproine) and acceptor levels.

Basically, the luminescent complexes showed a similar photoluminescence trend both in aqueous solution and in the SiO_2 glassy layers, indicating that the phenanthroline derivatives (**19** and **15**) and the acetophenone-based units (**18**), resulted to be the most efficient antenna systems for the Eu^{3+} and Tb^{3+} luminescence respectively, irrespective of the chromophore amount and thermal annealing.

All samples, when irradiated with a UV light (λ = 254 and 365 nm, 4 W tubes), presented a bright red (Eu^{3+}) or green (Tb^{3+}) luminescence clearly visible at the naked eye. Furthermore, whereas the luminescence quantum yield and lifetime are not influenced by the different conditions, the difference in the emission intensities between diluted (1 Ln^{3+}: 400 Si) and concentrated (1 Ln^{3+}: 100 Si) solid samples was clearly appreciated also at macroscopic level. Furthermore, antenna complexes, simply dispersed *via* sol–gel and not covalently linked to the SiO_2 matrix, showed a uniform distribution inside the glassy layers, similar to that found for the covalently linked analogues [126,127]. Irrespective of the structural difference of the employed chromophores and their concentration in the sol–gel silica matrices, similar in-depth distribution features are evidenced from secondary ion mass spectrometry (SIMS) profiles. Interestingly, the chemical analysis (X-ray Photoelectron Spectroscopy, XPS) pointed out, together with SIMS results, the integrity of the complexes and the efficacy of the employed synthesis strategy for the realization of highly dispersed *host–guest* systems. We observed that the overall luminescence quantum yields of the films were high and only slightly affected by the nature of the *host–guest* chemical interactions between the matrix and the chromophores. Consequently, whenever the synthesis of antenna complexes suitably functionalized for the covalent linking to the *host* medium is very demanding or almost impossible to be achieved, comparable luminescent efficiencies can be obtained by embedding the proper luminescent molecular components into transparent host matrices. Hence, for solid-state lighting purposes, the choice between covalent grafting *vs.* embedding of the complexes will be driven, once identified the best sensitizer, by the possibility of an easy functionalization procedure for the antenna unit.

In a different study [126] concerning the possibility to develop silica glassy layers with controlled and ready colour tunabilities, the specific case of films incorporating both Eu and Tb antenna derivatives is subsequently outlined. Employing a unique dipartite ligand, consisting of DO3A acting as chelating "cage" and an acetophenone unit (the antenna) functionalized with propyl-hydroxy group [126,127], highly luminescent silica-based thin films embedding $Eu^{3+} \subset$ **20** and $Tb^{3+} \subset$ **20** have been prepared. To modulate the colour output, solutions containing variable $Tb^{3+} \subset$ **20**/$Eu^{3+} \subset$ **20** molar ratios were used. This approach allowed us to obtain Eu_2–Tb_1, Eu_1–Tb_1 and Eu_1–Tb_2 hybrids, featuring Tb/Eu molar ratio of 0.4, 1.0 and 2.2 respectively.

The random distribution of the chromophores into the matrix results in a homogeneous colour output and upon changing the ratio between metal complexes within the SiO_2 *host* the resulting colour changes from red (Eu), to intermediate colours (Eu_2–Tb_1, Eu_1–Tb_1 and Eu_1–Tb_2), and finally to green (Tb), without eye-appreciable colour heterogeneity (Fig. 19).

As can be seen from Table 4 each type of emitter maintains its luminescence properties within the silica matrix. As a result, the produced colours arise from the statistical mixing of the green and red emissions and were shown to include degrees of pale yellow not far from white emission.

These hybrid materials show attractive properties from both the mechanical and chemical viewpoints, and the doping of different inorganic matrices with lanthanide complexes emitting in the visible range represents a promising way to fabricate a variety of luminescent and electro-luminescent devices. Along these lines, we are investigating the use of further blue-greenish emitters to afford white-light emitting single layers obtained through easy-manageable synthesis of photoactive materials and simple fabrication processes.

6. Conclusions

The research in the area of luminescent lanthanide complexes is steadily growing mainly because of their unique optical and magnetic properties that find application in many technologically interesting fields ranging from lasers and white light generation to optical fibre for telecommunication to biological Time Resolved FluoroImmunoAssays (TR-FIA). In order to correctly approach this research it is necessary to know: (i) the basic principles of rare-earth elements e.g. the electronic properties that are at the origin of their unique optical behaviour; (ii) the coordination features of the Ln^{3+} cations and the aspects that allow the design of ligands whose complexes have to show optimized luminescent properties; (iii) the basic concepts that rule the photophysical properties of luminescent lanthanide complexes; (iv) the basic concepts necessary to design highly stable and homogeneous materials that allow to transfer the results of the research to the daily life used macroscopic devices.

Our effort in writing this paper was to give, although not exhaustively, an answer to all these issues with the aim of contributing both to the enhancement of basic research and to the development of new and better performing materials and devices.

Acknowledgements

This work was financially supported by EC (IST-2002-004607, OLLA), CNR, MIUR and MSE (FIRB RBNE033KMA "Molecular compounds and hybrid nanostructured materials with resonant and non-resonant optical properties for photonic devices"; PROMO CNR-INSTM; CARIPARO 2006 "Multi-layer optical devices based on inorganic and hybrid materials by innovative synthetic strategies"; Industria 2015, ALADIN).

References

[1] J. Emsley, Nature's Building Blocks An A–Z Guides to the Elements, Oxford University Press, 2003.
[2] C. Baskerville, Science 19 (1904) 88.
[3] J.C.G. Bunzli, C. Piguet, Chem. Soc. Rev. 34 (2005) 1048.
[4] C.K. Jørgensen, The Inner Mechanism of Rare Earths Elucidated by Photo-Electron Spectra, Springer, Berlin/Heidelberg, 1973.
[5] I. McGill, Rare Earth Elements, Wiley-VCH Verlag GmbH & Co., KGaA, Weinheim, 2005.
[6] M.E. Weeks, J. Chem. Educ. 9 (1932) 1751.
[7] V.W.W. Yam, K.K.W. Lo, Coord. Chem. Rev. 184 (1999) 157.
[8] S. Aime, S.G. Crich, E. Gianolio, G.B. Giovenzana, L. Tei, E. Terreno, Coord. Chem. Rev. 250 (2006) 1562.
[9] C. Benelli, D. Gatteschi, Chem. Rev. 102 (2002) 2369.
[10] S.G. Crich, L. Biancone, V. Cantaluppi, D.D.G. Esposito, S. Russo, G. Camussi, S. Aime, Magn. Reson. Med. 51 (2004) 938.
[11] G.M. Davies, S.J.A. Pope, H. Adams, S. Faulkner, M.D. Ward, Inorg. Chem. 44 (2005) 4656.
[12] S. Aime, M. Botta, D. Parker, J.A.G. Williams, J. Chem. Soc., Dalton Trans. (1996) 17.
[13] J.C.G. Bunzli, Acc. Chem. Res. 39 (2006) 53.
[14] C.M.G. dos Santos, P.B. Fernandez, S.E. Plush, J.P. Leonard, T. Gunnlaugsson, Chem. Commun. (2007) 3389.
[15] D.D. Castelli, E. Gianolio, S.G. Crich, E. Terreno, S. Aime, Coord. Chem. Rev. 252 (2008) 2424.
[16] A. Beeby, S.W. Botchway, I.M. Clarkson, S. Faulkner, A.W. Parker, D. Parker, J.A.G. Williams, J. Photochem. Photobiol. B: Biol. 57 (2000) 83.
[17] S. Faulkner, S.J.A. Pope, B.P. Burton-Pye, Appl. Spectros. Rev. 40 (2005) 1.
[18] S.I. Klink, G.A. Hebbink, L. Grave, F. Van Veggel, D.N. Reinhoudt, L.H. Slooff, A. Polman, J.W. Hofstraat, J. Appl. Phys. 86 (1999) 1181.
[19] B.H. Bakker, M. Goes, N. Hoebe, H.J. Van Ramesdonk, J.W. Verhoeven, M.H.V. Werts, J.W. Hofstraat, Coord. Chem. Rev. 208 (2000) 3.
[20] T.J. Foley, B.S. Harrison, A.S. Knefely, K.A. Abboud, J.R. Reynolds, K.S. Schanze, J.M. Boncella, Inorg. Chem. 42 (2003) 5023.
[21] S. Quici, M. Cavazzini, G. Marzanni, G. Accorsi, N. Armaroli, B. Ventura, F. Barigelletti, Inorg. Chem. 44 (2005) 529.
[22] S. Quici, G. Marzanni, A. Forni, G. Accorsi, F. Barigelletti, Inorg. Chem. 43 (2004) 1294.
[23] D. Guo, C.Y. Duan, F. Lu, Y. Hasegawa, Q.J. Meng, S. Yanagida, Chem. Commun. (2004) 1486.
[24] S. Faulkner, S.J.A. Pope, J. Am. Chem. Soc. 125 (2003) 10526.
[25] R.S. Dickins, S. Aime, A.S. Batsanov, A. Beeby, M. Botta, J. Bruce, J.A.K. Howard, C.S. Love, D. Parker, R.D. Peacock, H. Puschmann, J. Am. Chem. Soc. 124 (2002) 12697.
[26] G.A. Hebbink, S.I. Klink, L. Grave, P.G.B.O. Alink, F.C.J.M. Van Veggel, Chemphyschem 3 (2002) 1014.
[27] I.A. Kamenskikh, N. Guerassimova, C. Dujardin, N. Garnier, G. Ledoux, C. Pedrini, M. Kirm, A. Petrosyan, D. Spassky, Opt. Mater. 24 (2003) 267.
[28] W.K. Wong, H.Z. Liang, W.Y. Wong, Z.W. Cai, K.F. Li, K.W. Cheah, New J. Chem. 26 (2002) 275.
[29] N.M. Shavaleev, S.J.A. Pope, Z.R. Bell, S. Faulkner, M.D. Ward, Dalton Trans. (2003) 808.
[30] Y. Oshishi, T. Kanamori, T. Kitagawa, S. Takashashi, E. Snitzer, G.H. Sigel, Opt. Lett. 16 (1991) 1747.
[31] L.H. Slooff, A. Polman, M.P.O. Wolbers, F. van Veggel, D.N. Reinhoudt, J.W. Hofstraat, J. Appl. Phys. 83 (1998) 497.
[32] A. Heller, J. Am. Chem. Soc. 89 (1967) 167.
[33] K. Kuriki, Y. Koike, Y. Okamoto, Chem. Rev. 102 (2002) 2347.
[34] K. Nakamura, Y. Hasegawa, H. Kawai, N. Yasuda, N. Kanehisa, Y. Kai, T. Nagamura, S. Yanagida, Y. Wada, The J. Phys. Chem. A 111 (2007) 3029.
[35] A. Beeby, L.M. Bushby, D. Maffeo, J.A.G. Williams, J. Chem. Soc., Dalton Trans. 1 (2002) 48.
[36] L.D. Carlos, R.A.S. Ferreira, V.D. Bermudez, C. Molina, L.A. Bueno, S.J.L. Ribeiro, Phys. Rev. B 60 (1999) 10042.
[37] T. Moeller, J. Chem. Educ. 47 (1970) 417.
[38] S.A. Cotton, Lanthanide and Actinide Chemistry, John Wiley & Sons, West Sussex, 2006.
[39] G. Malandrino, I.L. Fragalà, Coord. Chem. Rev. 250 (2006) 1605.
[40] R.D. Shannon, Acta Crystallog. Sect. A A32 (1976) 751.
[41] M. Seitz, A.G. Oliver, K.N. Raymond, J. Am. Chem. Soc. 129 (2007) 11153.
[42] E.N. Rizkalla, Radiochim. Acta 61 (1993) 181.
[43] J.A. Peters, J. Huskens, D.J. Raber, Prog. Nucl. Magn. Reson. Spectrosc. 28 (1996) 283.
[44] T. Kurisaki, T. Yamaguchi, H. Wakita, J. Alloys Compd. 192 (1993) 293.
[45] H. Kanno, H. Yokoyama, Polyhedron 15 (1996) 1437.
[46] T. Kowall, F. Foglia, L. Helm, A.E. Merbach, J. Am. Chem. Soc. 117 (1995) 3790.
[47] C. Cossy, L. Helm, D.H. Powell, A.E. Merbach, New J. Chem. 19 (1995) 27.
[48] D.C. Bradley, J.S. Ghotra, F.A. Hart, J. Chem. Soc., Dalton Trans. 10 (1973) 1021.
[49] H.C. Aspinall, M.R. Tillotson, Polyhedron 13 (1994) 3229.
[50] F.A. Cotton, G. Wilkinson, C.A. Murillo, M. Bochmann, Advanced Inorganic Chemistry, 6th ed., John Wiley & Sons Ltd., New York, 1999.
[51] M. Montalti, A. Credi, L. Prodi, M.T. Gandolfi, Handbook of Photochemistry, 3rd ed., CRC Press, Taylor & Francis, Boca Raton, 2006.
[52] N. Sabbatini, M. Guardigli, J.M. Lehn, Coord. Chem. Rev. 123 (1993) 201.
[53] N. Sabbatini, M. Guardigli, I. Manet, Handbook Phys. Chem. Rare Earths, Elsevier, Amsterdam, 1996.
[54] T. Lazarides, G.M. Davies, H. Adams, C. Sabatini, F. Barigelletti, A. Barbieri, S.J.A. Pope, S. Faulkner, M.D. Ward, Photochem. Photobiol. Sci. 6 (2007) 1152.
[55] M.D. Ward, Coord. Chem. Rev. 251 (2007) 1663.
[56] T.K. Ronson, T. Lazarides, H. Adams, S.J.A. Pope, D. Sykes, S. Faulkner, S.J. Coles, M.B. Hursthouse, W. Clegg, R.W. Harrington, M.D. Ward, Chem.-Eur. J. 12 (2006) 9299.
[57] H.B. Xu, L.X. Shi, E. Ma, L.Y. Zhang, Q.H. Wei, Z.N. Chen, Chem. Commun. (2006) 1601.
[58] J.-M. Herrera, M.D. Ward, H. Adams, S.J.A. Pope, S. Faulkner, Chem. Commun. (2006) 1851.
[59] S.I. Klink, H. Keizer, F.C.J.M. Van Veggel, Angew. Chem. Int. Ed. 39 (2000) 4319.
[60] S. Sato, M. Wada, Bull. Chem. Soc. Jpn. 43 (1970) 1955.
[61] M. Tanaka, G. Yamaguchi, J. Shiokawa, Bull. Chem. Soc. Jpn. 43 (1970) 549.
[62] A.V. Hayes, H.G. Drickamer, J. Chem. Phys. 76 (1982) 114.
[63] W.D. Horrocks, D.R. Sudnick, Acc. Chem. Res. 14 (1981) 384.
[64] A. Beeby, I.M. Clarkson, R.S. Dickins, S. Faulkner, D. Parker, L. Royle, A.S. De Sousa, J.A.G. Williams, M. Woods, J. Chem. Soc., Perkin Trans. 2 (3) (1999) 493.
[65] M.J. Weber, Phys. Rev. 171 (1968) 283.
[66] M.H.V. Werts, R.T.F. Jukes, J.W. Verhoeven, Phys. Chem. Chem. Phys. 4 (2002) 1542.
[67] D. Parker, Coord. Chem. Rev. 205 (2000) 109.
[68] J.-M. Lehn, Design of Organic Complexing Agents Strategies Towards Properties, Springer, Berlin, Heidelberg, 1973.
[69] R. Englman, J. Jortner, Mol. Phys. 18 (1970) 145.
[70] J.V. Caspar, T.J. Meyer, J. Am. Chem. Soc. 105 (1983) 5583.
[71] M. Latva, H. Takalo, V.-M. Mukkala, C. Matachescu, J.C. Rodriguez-Ubis, J. Kankare, J. Lumin. 75 (1997) 149.
[72] T. Förster, Discuss. Faraday Soc. 27 (1959) 7.
[73] D.L. Dexter, J. Chem. Phys. 21 (1952) 836.
[74] A. Juris, V. Balzani, F. Barigelletti, S. Campagna, P. Belser, A. Von Zelewsky, Coord. Chem. Rev. 84 (1988) 85.
[75] J.P. Sauvage, J.P. Collin, J.C. Chambron, S. Guillerez, C. Coudret, V. Balzani, F. Barigelletti, L. De Cola, L. Flamigni, Chem. Rev. 94 (1994) 993.
[76] E. Bardez, I. Devol, B. Larry, B. Valeur, J. Phys. Chem. B 101 (1997) 7786.
[77] A.P.S. Samuel, E.G. Moore, M. Melchior, J. Xu, K.N. Raymond, Inorg. Chem. 47 (2008) 7535.
[78] E.G. Moore, J. Xu, C.J. Jocher, I. Castro-Rodriguez, K.N. Raymond, Inorg. Chem. 47 (2008) 3105.
[79] M. Albrecht, M. Fiege, O. Osetska, Coord. Chem. Rev. 252 (2008) 812.
[80] F. Vögtle, E. Weber, Angew. Chem. Int. Ed. 18 (1979) 753.
[81] N. Marques, A. Sella, J. Takats, Chem. Rev. 102 (2002) 2137.

[82] N. Armaroli, G. Accorsi, F. Barigelletti, S.M. Couchman, J.S. Fleming, N.C. Harden, J.C. Jeffery, K.L.V. Mann, J.A. McCleverty, L.H. Rees, S.R. Starling, M.D. Ward, Inorg. Chem. 38 (1999) 5769.
[83] E. Brunet, O. Juanes, J.C. Rodriguez-Ubis, Curr. Chem. Biol. 1 (2007) 11.
[84] E.G. Moore, A.P.S. Samuel, K.N. Raymond, Acc. Chem. Res. 42 (2009) 542.
[85] K.W.-Y. Chan, W.-T. Wong, Coord. Chem. Rev. 251 (2007) 2428.
[86] P. Caravan, J.J. Ellison, T.J. McMurry, R.B. Lauffer, Chem. Rev. 99 (1999) 2293.
[87] P.G. Sammes, G. Yahioglu, Nat. Prod. Rep. 13 (1996) 1.
[88] M. Li, P.R. Selvin, J. Am. Chem. Soc. 117 (1995) 8132.
[89] H. Hakala, P. Liitti, J. Peuralahti, J. Karvinen, V.-M. Mukkala, J. Hovinen, J. Lumin. 113 (2005) 17.
[90] I. Hemmila, V.-M. Mukkala, Crit. Rev. Clin. Lab. Sci. 38 (2001) 441.
[91] P.R. Selvin, Annu. Rev. Biophys. Biomol. Struct. 31 (2002) 275.
[92] D.E. Reichert, J.S. Lewis, C.J. Anderson, Coord. Chem. Rev. 184 (1999) 3.
[93] R.M. Izatt, K. Pawlak, J.S. Bradshaw, R.L. Bruening, Chem. Rev. 91 (1991) 1721.
[94] S. Aime, A.S. Batsanov, M. Botta, J.A.K. Howard, D. Parker, K. Senanayake, G. Williams, Inorg. Chem. 32 (1994) 4696.
[95] A. Nonat, C. Gateau, P.H. Fries, M. Mazzanti, Chem. -Eur. J. 12 (2006) 7133.
[96] E. Balogh, R. Tripier, P. Fouskova, F. Reviriego, H. Handel, E. Toth, Dalton Trans. 32 (2007) 3572.
[97] S. Quici, G. Marzanni, M. Cavazzini, P.L. Anelli, M. Botta, E. Gianolio, G. Accorsi, N. Armaroli, F. Barigelletti, Inorg. Chem. 41 (2002) 2777.
[98] S. Quici, M. Cavazzini, M.C. Raffo, M. Botta, G.B. Giovenzana, B. Ventura, G. Accorsi, F. Barigelletti, Inorg. Chim. Acta 360 (2007) 2549.
[99] F. Barigelletti, L. Flamigni, Chem. Soc. Rev. 29 (2000) 1.
[100] A.F. Kirby, F.S. Richardson, J. Phys. Chem. 87 (1983) 2544.
[101] C.M.G. dos Santos, A.J. Harte, S.J. Quinn, T. Gunnlaugsson, Coord. Chem. Rev. 252 (2008) 2512.
[102] L.D. Carlos, R.A.S. Ferreira, V. de Zea Bermudez, S.J.L. Ribeiro, Adv. Mater. 21 (2009) 509.
[103] H.R. Li, N.N. Lin, Y.G. Wang, Y. Feng, Q.Y. Gan, H.J. Zhang, Q.L. Dong, Y.H. Chen, Eur. J. Inorg. Chem. (2009) 519.
[104] C. Sanchez, G.J.A.A. Soler-Illia, F. Ribot, D. Grosso, C.R. Chim. 6 (2003) 1131.
[105] T. Coradin, J. Livage, Acc. Chem. Res. 40 (2007) 819.
[106] P. Escribano, B. Julian-Lopez, J. Planelles-Arago, E. Cordoncillo, B. Viana, C. Sanchez, J. Mater. Chem. 18 (2008) 23.
[107] T. Nishioka, J. Yuan, Y. Yamamoto, K. Sumitomo, Z. Wang, K. Hashino, C. Hosoya, K. Ikawa, G. Wang, K. Matsumoto, Inorg. Chem. 45 (2006) 4088.
[108] E. Soini, T. Lovgren, Crit. Rev. Anal. Chem. 18 (1987) 105.
[109] E.F. Dickson Gudgin, A. Pollak, E.P. Diamandis, Pharmacol. Ther. 66 (1995) 207.
[110] K. Matsumoto, J. Yuan, in: A.S.a.H Sigel (Ed.), Metal Ions in Biological Systems, vol. 40, Marcel Dekker, New York, 2003, p. 191.
[111] A.-C. Ferrand, D. Imbert, A.-S. Chauvin, C.D.B. Vandevyver, J.-C.G. Buenzli, Chem. -Eur. J. 13 (2007) 8678.
[112] A.J. Wilkinson, D. Maffeo, A. Beeby, C.E. Foster, J.A.G. Williams, Inorg. Chem. 46 (2007) 9438.
[113] J. Yuan, G. Wang, J. Fluo. 15 (2005) 559.
[114] I. Hemmilä, E. Soini, Clin. Chem. 25 (1979) 353.
[115] R.P. Bagwe, C. Yang, L.R. Hilliard, W. Tan, Langmuir 20 (2004) 8336.
[116] J. Yan, M.C. Estévez, J.E. Smith, K. Wang, X. He, L. Wang, W. Tan, Nano Today 2 (2007) 44.
[117] J.E. Smith, L. Wang, W. Tan, Trends Anal. Chem. 25 (2006) 848.
[118] R.P. Bagwe, L.R. Hilliard, W. Tan, Langmuir 22 (2006) 4357.
[119] W. Tan, K. Wang, X. He, X.J. Zhao, T. Drake, L. Wang, R.P. Bagwe, Med. Res. Rev. 24 (2004) 621.
[120] H.K. Kim, S.-J. Kang, S.-K. Choi, Y.-H. Min, C.-S. Yoon, Chem. Mater. 11 (1999) 779.
[121] L.N. Sun, H.J. Zhang, L.S. Fu, F.Y. Liu, Q.G. Meng, C.Y. Peng, J.B. Yu, Adv. Funct. Mater. 15 (2005) 1041.
[122] J. Kido, Y. Okamoto, Chem. Rev. 102 (2002) 2357.
[123] Y. Li, B. Yan, H. Yang, J. Phys. Chem. C 112 (2008) 3959.
[124] P.A. Tanner, B. Yan, H. Zhang, J. Mater. Sci. 35 (2000) 4325.
[125] N.I. Koslova, B. Viana, C. Sanchez, J. Mater. Chem. 3 (1993) 111.
[126] L. Armelao, G. Bottaro, S. Quici, M. Cavazzini, M.C. Raffo, F. Barigelletti, G. Accorsi, Chem. Commun. 28 (2007) 2911.
[127] S. Quici, M. Cavazzini, M.C. Raffo, L. Armelao, G. Bottaro, G. Accorsi, C. Sabatini, F. Barigelletti, J. Mater. Chem. 16 (2006) 741.
[128] C. Sanchez, B. Lebeau, MRS Bull. 26 (2001) 377.
[129] R. Gupta, N.K. Chaudhury, Biosens. Bioelectron 22 (2007) 2387.
[130] O. Lev, M. Tsionsky, L. Rabinovich, V. Glezer, S. Sampath, I. Pankratov, J. Gun, Anal. Chem. 67 (1995) 22A.
[131] L.M. Ellerby, C.R. Nishida, F. Nishida, S.A. Yamanaka, B. Dunn, J.S. Valentine, J.I. Zink, Science 255 (1992) 1113.
[132] T. Keeling-Tucker, J.D. Brennan, Chem. Mater. 13 (2001) 3331.
[133] A.-L. Penard, T. Gacoin, J.-P. Boilot, Acc. Chem. Res. 40 (2007) 895.
[134] C.J. Brinker, G.W. Scherer, Sol–Gel Science: The Physics and Chemistry of Sol–Gel Processing, Academic Press Inc., San Diego, 1990.
[135] U. Schubert, N. Hüsing, Synthesis of Inorganic Materials, Wiley-VCH, Chichester, 2000.
[136] L. Armelao, D. Barreca, G. Bottaro, A. Gasparotto, E. Tondello, M. Ferroni, S. Polizzi, Chem. Vap. Deposition 10 (2004) 257.
[137] L. Armelao, D. Barreca, G. Bottaro, A. Gasparotto, E. Tondello, M. Ferroni, S. Polizzi, Chem. Mater. 16 (2004) 3331.
[138] S. Quici, C. Scalera, M. Cavazzini, G. Accorsi, M. Bolognesi, L. Armelao, G. Bottaro, Chem. Mater. 21 (2009) 2941.